Inorg. Chem. **2006**, *45*, 4214–4227

Diastereopure Fe(II) and Zn(II) Complexes Derived from a Tridentate *N,N′,N*-Bis(methyl-L-prolinate)-Substituted Pyridine Ligand

Silvia Gosiewska,[†] Jeroen J. L. M. Cornelissen,[⊥] Martin Lutz,[‡] Anthony L. Spek,[‡,§] Gerard van Koten,[†] and Robertus J. M. Klein Gebbink*[,†]

Debye Institute, Organic Chemistry and Catalysis, Utrecht University, Padualaan 8, 3584 CH Utrecht, The Netherlands, Bijvoet Center for Biomolecular Research, Crystal and Structural Chemistry, Utrecht University, Padualaan 8, 3584 CH Utrecht, The Netherlands, and Department of Organic Chemistry, Radboud University at Nijmegen, Toernooiveld 1, 6525 ED Nijmegen, The Netherlands

Received January 23, 2006

A series of mononuclear iron(II) and zinc(II) complexes of the new chiral **Py(ProMe)$_2$** ligand (**Py(ProMe)$_2$** = 2,6-bis[[(*S*)-2-(methyloxycarbonyl)-1-pyrrolidinyl]methyl]pyridine) have been prepared. The molecular geometry in the solid state (X-ray crystal structures) of the complexes [$FeCl_2$(**Py(ProMe)$_2$**)] (**1**), [$ZnCl_2$(**Py(ProMe)$_2$**)] (**2**), [Fe($OTf)_2$-(**Py(ProMe)$_2$**)] (**3**), [Fe(**Py(ProMe)$_2$**)($OH_2)_2$]($OTf)_2$ (**4**), and [Zn(OTf)(**Py(ProMe)$_2$**)](OTf) (**5**) are reported. They all show a meridional NN′N coordination of the **Py(ProMe)$_2$** ligand. The bis-chloride derivatives **1** and **2** represent neutral isostructural five-coordinated complexes with a distorted geometry around the metal center. Unusual seven-coordinate iron(II) complexes **3** and **4** having a pentagonal bipyramidal geometry were obtained using weakly coordinating triflate anions. The reaction of $Zn(OTf)_2$ with the **Py(ProMe)$_2$** ligand afforded complex **5** with a distorted octahedral geometry around the zinc center. All complexes were formed as single diastereoisomers. In the case of complexes **3**–**5**, the oxygen atoms of both carbonyl groups of the ligand are also coordinated to the metal. The stereochemistry of the coordinated tertiary amine donors in complexes **3**–**5** is of opposite configuration as in complexes **1** and **2** as a result of the planar penta-coordination of the ligand **Py(ProMe)$_2$**. Complexes **1**, **2**, and **5** have an overall Λ-configuration at their metal center, while the Fe(II) ion in complexes **3** and **4** has the opposite Δ-configuration (crystal structures and CD measurements). The magnetic moments of iron complexes **1**, **3**, and **4** correspond to that of high-spin d^6 Fe(II) complexes. The solution structures of complexes **1**–**5** were characterized by means of UV–vis, IR, conductivity, and CD measurements and their electrochemical behavior. These studies showed that the coordination environment of **1** and **2** observed in the solid state is maintained in solution. In coordinating solvents, the triflate anion (**3**, **5**) or water (**4**) co-ligands of complexes **3**–**5** are replaced by solvent molecules with retention of the original pentagonal bipyramidal and octahedral geometry, respectively.

Introduction

The selective oxidation of unfunctionalized hydrocarbons, using environmentally friendly oxidants such as O_2 and H_2O_2 still represents a major challenge in synthetic chemistry.[1,2] Biological systems play an important inspirational role in the design of new catalysts for such transformations.[3] Extensive research efforts are currently devoted to the synthesis of models for the active sites of metalloenzymes that are able to activate dioxygen to oxidize exogenous substrates.[4b] Various non-heme iron complexes based on polydentate nitrogen donor ligands have been reported for the oxidation of organic substrates using a variety of oxidants (O_2, H_2O_2, ROOH, etc.).[4] Ligands that are widely used in

* To whom correspondence should be addressed. E-mail: r.j.m.kleingebbink@chem.uu.nl. Phone: +31-30-2531889. Fax: +31-302523615.

§ To whom correspondence pertaining to crystallographic studies should be addressed. E-mail: a.l.spek@chem.uu.nl. Phone: +31-30-2532538. Fax: +31-30-2533940.

† Debye Institute, Organic Chemistry and Catalysis, Utrecht University.

‡ Bijvoet Center for Biomolecular Research, Crystal and Structural Chemistry, Utrecht University.

⊥ Radboud University at Nijmegen.

(1) Sheldon, R. A.; Kochi, J. K. *Metal-Catalyzed Oxidations of Organic Compounds*; Academic Press: New York, 1981.

(2) Bäckvall, J.-E. *Modern Oxidation Methods*; Wiley-VCH: Weinheim, 2004.

(3) Meunier, B. *Biomimetic Oxidations Catalyzed by Transition Metal Complexes*; Imperial College Press: London, 1999.

10.1021/ic060134z CCC: $33.50
Published on Web 04/21/2006

these complexes include pentadentate *N*,*N*-bis(2-pyridylmethyl)-*N*-bis(2-pyridyl)methylamine (N4Py),[5] tetradentate tris(2-pyridylmethyl)amine (TPA),[6] *N*,*N*′-bis-(2-pyridylmethyl)-*N*,*N*′-dimethyl-1,2-ethylenediamine (BPMEN),[7,6e,f,9] derivatives of 1,4,8,11-tetraazacyclotetradecane (cyclam)[8] and (*R*,*R*)-*N*,*N*′-bis-(2-pyridylmethyl)-*N*,*N*′-dimethyl-1,2-cyclohexanediamine (BPMCN),[9] and tridentate 1,4,7-triazacyclononane (TACN).[10] Except for the cyclam ligand, these multidentate nitrogen ligands facially cap the metal center, which contains one or two additional labile co-ligands, L (Figure 1). Interesting results were obtained with these systems in alkene and/or alkane oxidation with H_2O_2 as oxidant yielding products formed via a metal-based mechanism rather than via an unselective radical chain autoxidation mechanism (Fenton chemistry).[11,12]

Metal complexes of tridentate nitrogen donor ligands have received much less attention in non-heme iron chemistry. Only recently were the synthesis and catalytic properties reported of a series of metal complexes containing either 2,6-bis(benzimidazol-2-yl)pyridine,[13] 2,6-bis(imino)pyridine, or 2,6-bis(amino)pyridine[14] ligands (Figure 1). Whereas the other ligands facially bind to a metal center, these ligands bind the metal ion in a meridional fashion. One aspect of the oxidation chemistry of metalloenzymes is the fact that most biological systems are intrinsically chiral. However, the use of chiral ligands to achieve oxidative transformations in an enantioselective manner has been largely overshadowed by the search for chemoselective catalysts. One notable exception is the (*R*,*R*)-BPMCN ligand, see Figure 1.[9]

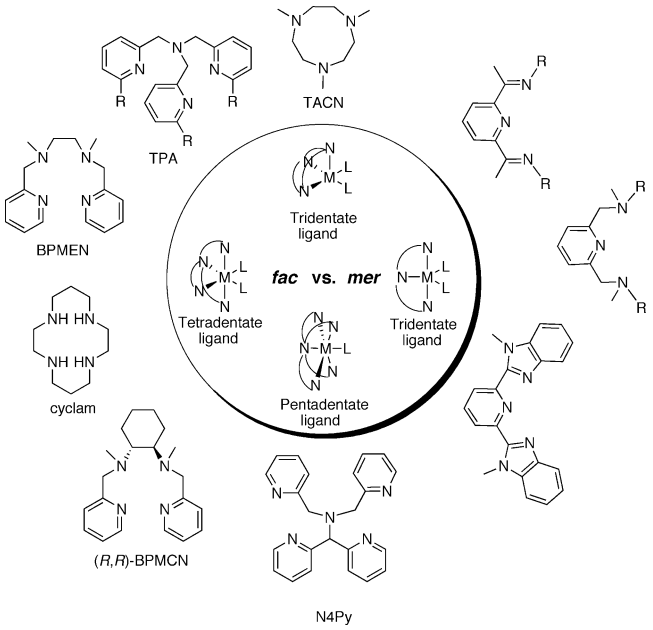

Figure 1. Examples of polydentate nitrogen ligands and their binding mode in non-heme iron complexes.

To examine the use of a chiral *N*,*N*′,*N*-tridentate coordinating ligand with a meridional ligation mode on the stereoselectivity of oxidation reactions, we have set out to investigate the coordination chemistry of 2,6-bis[[(*S*)-2-(methyloxycarbonyl)-1-pyrrolidinyl]methyl]pyridine **Py(ProMe)$_2$** (Scheme 1). Next to one pyridyl nitrogen and two proline-derived aliphatic nitrogen donors, this ligand comprises two prolinate ester moieties for which we envisioned an additional coordinating and activating role.[15] Moreover, this ligand is chiral through the presence of the two methyl-L-prolinate substituents. The stereochemical information of commercially available prolinate esters, enantiomerically pure building blocks of great utility, can be retained by choosing appropriate reaction conditions during both synthesis and purification of their metal complexes. Here, we describe a study of the coordination behavior of the **Py(ProMe)$_2$** ligand toward zinc(II) and iron(II) salts and of the influence of the coordination ability of counteranions on the geometry of the resulting metal complexes. The structures in the solid state and in solution of these complexes are presented, as well as their stereochemistry and physical properties. The numbering used

(4) For reviews, see: (a) Costas, M.; Chen, K.; Que, L., Jr. *Coord. Chem. Rev.* **2000**, *200*−*202*, 517−544. (b) Costas, M.; Mehn, M. P.; Jensen, M. P.; Que, L., Jr. *Chem. Rev.* **2004**, *104*, 939−986. (c) Kryatov, S. V.; Rybak-Akimova, E. V.; Schindler, S. *Chem. Rev.* **2005**, *105*, 2175−2226.

(5) (a) Lubben, M.; Meetsma, A.; Wilkinson, E. C.; Feringa, B. L.; Que, L., Jr. *Angew. Chem., Int. Ed. Engl.* **1995**, *34*, 1512−1514. (b) Roelfes, G.; Lubben, M.; Leppard, S. W.; Schudde, E. P.; Hermant, R. M.; Hage, R.; Wilkinson, E. C.; Que, L., Jr.; Feringa, B. L. *J. Mol. Catal. A: Chem.* **1997**, *117*, 223−227. (c) Roelfes, G.; Lubben, M.; Hage, R.; Que, L., Jr.; Feringa, B. L. *Chem. Eur. J.* **2000**, *6*, 12, 2152−2159. (d) Roelfes, G.; Vrajmasu, V.; Chen, K.; Ho, R. Y. N.; Rohde, J.-U.; Zondervan, Ch.; la Crois, R. M.; Schudde, E. P.; Lutz, M.; Spek, A. L.; Hage, R.; Feringa, B. L.; Munck, E.; Que, L., Jr. *Inorg. Chem.* **2003**, *42*, 2639−2653. (e) van den Berg, T. A.; de Boer, J. W.; Browne, W. R.; Roelfes, G.; Feringa, B. L. *Chem. Commun.* **2004**, 2550−2551.

(6) (a) Dong, Y.; Fujii, H.; Hendrich, M. P.; Leising, R. A.; Pan, G.; Randall, C. R.; Wilkinson, E. C.; Zang, Y.; Que, L., Jr.; Fox, B. G.; Kauffmann, K.; Münck, E. *J. Am. Chem. Soc.* **1995**, *117*, 2778−2792. (b) Zang, Y.; Kim, J.; Dong, Y.; Wilkinson, E. C.; Appelman, E. H.; Que, L., Jr. *J. Am. Chem. Soc.* **1997**, *119*, 4197−4205. (c) Kim, C.; Chen, K.; Kim, J.; Que, L., Jr. *J. Am. Chem. Soc.* **1997**, *119*, 5964−5965. (d) Chen, K.; Que, L., Jr. *J. Am. Chem. Soc.* **2001**, *123*, 6327−6337. (e) Chen, K.; Costas, M.; Kim, J.; Tipton, A.; Que, L., Jr. *J. Am. Chem. Soc.* **2002**, *124*, 3026−3035. (f) Ryu, J. Y.; Kim, J.; Costas, M.; Chen, K.; Nam, W.; Que, L., Jr. *Chem. Commun.* **2003**, 1288−1289.

(7) (a) Toflund, H.; Pedersen, E.; Yde-Andersen, S. *Acta Chem. Scand. A* **1984**, *38*, 693−697. (b) White, M. C.; Doyle, A. G.; Jacobsen, E. N. *J. Am. Chem. Soc.* **2001**, *123*, 7194−7195. (c) Balland, V.; Banse, F.; Anxolabéhère-Mallart, E.; Nierlich, M.; Girerd, J.-J. *Eur. J. Inorg. Chem.* **2003**, 2529−2535. For recent example of tetradentate ligands, see: (d) Mekmouche, Y.; Ménage, S.; Pécaut, J.; Lebrun, C.; Reilly, L.; Schuenemann, V.; Trautwein, A.; Fontecave, M. *Eur. J. Inorg. Chem.* **2004**, 3163−3171. (e) Britovsek, G. J. P.; England, J.; White, A. J. P. *Inorg. Chem.* **2005**, *44*, 8125−8134.

(8) (a) Nam, W.; Ho, R.; Valentine, J. S. *J. Am. Chem. Soc.* **1991**, *113*, 7052−7054. (b) Rohde, J. U.; In, J.-H.; Lim, M. H.; Brennessel, W. W.; Bukowski, M. R.; Stubna, A.; Münck, E.; Nam, W.; Que, L., Jr. *Science* **2003**, *299*, 1037−1039.

(9) Costas, M.; Tipton, A. K.; Chen, K.; Jo, D.-W.; Que, L., Jr. *J. Am. Chem. Soc.* **2001**, *123*, 6722−6723.

(10) (a) Wieghardt, K.; Pohl, K.; Gebert, W. *Angew. Chem., Int. Ed. Engl.* **1983**, *22*, 727. (b) Shul'pin, G. B.; Nizova, G. V.; Kozlov, Y. N.; Gonzales Cuervo, L.; Süss-Fink, G. *Adv. Synth. Catal.* **2004**, *346*, 317−332.

(11) Parallel screening of various ligands: Klopstra, M.; Hage, R.; Kellogg, R. M.; Feringa, B. L. *Tetrahedron Lett.* **2003**, *44*, 4581−4584.

(12) Some other interesting examples include: (a) Francis, M. B.; Jacobsen, E. N. *Angew. Chem., Int. Ed.* **1999**, *38*, 937−941. (b) Dubois, G.; Murphy, A.; Stack, T. D. P. *Org. Lett.* **2003**, *5*, 2569−2472.

(13) Wang, X.; Wang, S.; Li, L.; Sundberg, B.; Gacho, G. P. *Inorg. Chem.* **2003**, *42*, 7799−7808.

(14) Britovsek, G. J. P.; England, J.; Spitzmesser, S. K.; White, A. J. P.; Williams, D. J. *Dalton Trans.* **2005**, 945−955.

(15) For an early example, see: Van de Kuil, L.; Veldhuizen, Y. S. J.; Grove, D.; Zwikker, J. W.; Jenneskens, J. W.; Drenth, W.; Smeets, W. J. J.; Spek, A. L.; van Koten, G. *Recl. Trav. Chim. Pays-Bas* **1994**, *113*, 267−277.

Scheme 1. Synthesis of Ligand **Py(ProMe)$_2$** and the Corresponding Metal Complexes **1**−**5**

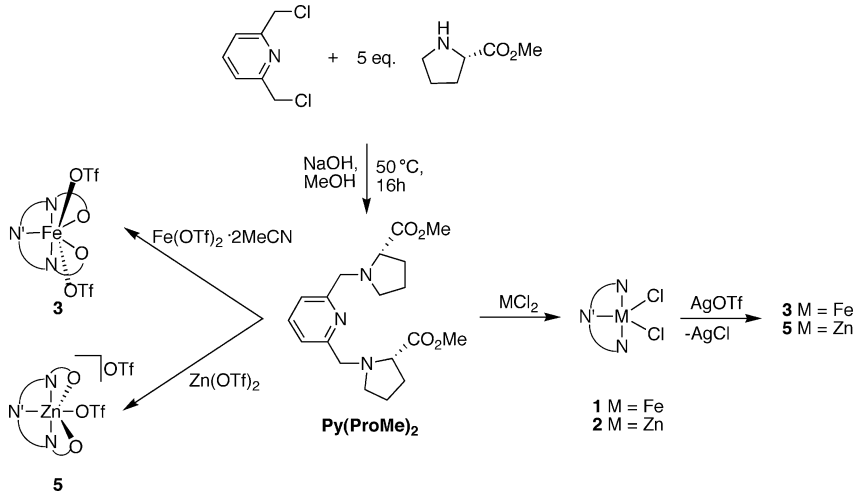

for the complexes discussed in this paper is shown in Chart 1.

Chart 1

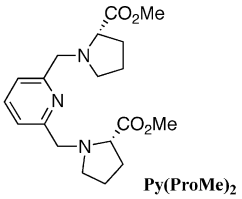

1 = [$FeCl_2$(**Py(ProMe)$_2$**)]
2 = [$ZnCl_2$(**Py(ProMe)$_2$**)]
3 = [$Fe(OTf)_2$(**Py(ProMe)$_2$**)]
4 = [Fe(**Py(ProMe)$_2$**)$(OH_2)_2$] $(OTf)_2$
5 = [Zn(OTf)(**Py(ProMe)$_2$**)] (OTf)

Experimental Section

Materials. Reactions with metal salts were carried out using standard Schlenk techniques. Solvents were dried and freshly distilled prior to use. Methyl-L-prolinate,[16] 2,6-bis(chloromethyl)-pyridine,[17] and $Fe(OTf)_2$·2MeCN[18] were prepared according to previously published procedures.

Instrumentation. ^{1}H (300.1 MHz) and $^{13}C\{^1H\}$ (75.5 MHz) NMR spectra were recorded on a Varian Inova 300 spectrometer. Optical rotations ($[\alpha]_D^{21}$) were measured with a Perkin polarimeter 241. Elemental microanalyses were carried out by Microanalytisches Laboratorium Dornis und Kolbe, Mulheim a.d. Ruhr, Germany. ESI-MS spectra were recorded on a Micromass LS-TOF mass spectrometer at the Bijvoet Institute, Biomolecular Mass Spectrometry, Utrecht University. Infrared spectra were recorded on a Perkin-Elmer Spectrum One FT-IR instrument. Solution IR spectra were recorded with a Mettler Toledo ReactIR 1000 spectrometer with a SiComp probe which was fitted in a reaction vessel under N_2 atmosphere. Solvent spectra were abstracted as a background. UV−vis spectra were recorded on a Carry 50 Varian spectrometer. CD spectra were recorded on a Jasco J810 instrument (Radboud University at Nijmegen). Magnetic moments of powdered samples at room temperature were measured using a Johnston Matthey Alfa products Mk1 magnetic susceptibility balance (Leiden Institute of Chemistry, Gorlaeous Laboratories) using Pascal's constants for diamagnetic corrections. Cyclic voltammetry (CV) was performed using an EG&G potentiostat/galvanostat model 263A in freshly distilled acetonitrile containing 0.1 M (*n*-BuN)PF_6 (Fluka) as supporting electrolyte at scanning rates of 50 and 100 ms^{-1} (potential window −2.5 to +2 V) and a $Ag/AgNO_3$ reference electrode. The potentials were referenced to Fc/Fc^+.

2,6-Bis[[(*S*)-2-(methyloxycarbonyl)-1-pyrrolidinyl]methyl]pyridine (Py(ProMe)$_2$). A solution of 2,6-bis(chloromethyl)pyridine (0.020 mol, 3.6 g) in MeOH (30 mL) was added to a solution of methyl-L-prolinate (0.1 mol, 13 g) dissolved in MeOH (50 mL). To the reaction mixture was added dropwise a solution of NaOH (0.12 mol, 4.9 g) in MeOH (50 mL), and the mixture was heated under reflux for 16 h. Subsequently, a white precipitate was filtered off and the filtrate was concentrated in vacuo. The remaining crude oil was purified via column chromatography (SiO_2, ethyl acetate/MeOH = 9:1 (v/v)). A yellow oil was obtained in 90% yield (6.57 g). Anal. Calcd for $C_{19}H_{27}N_3O_4$: C 63.14, H 7.53, N 11.63. Found: C 62.95, H 7.58, N 11.72. ESI-MS *m*/*z* 362.33 ($(M + H)^+$, calcd 362.21); $[\alpha]_D^{21}$ −65.07 deg cm^3 g^{-1} dm^{-1} (*c* 1.0, $CHCl_3$); IR (cm^{-1}, solid) ν 2951(m), 2818 (w), 1731 (s), 1590 (w), 1576 (w), 1456 (m), 1435 (m), 1359 (w), 1276 (w), 1196 (s), 1169 (s), 1036 (w), 994 (w), 764 (w); ^{1}H NMR ($CDCl_3$) δ 1.81−1.85 (m, 2H, CH_2 ring, γ to CO), 1.88−1.98 (m, 4H, CH_2 ring, β and γ to CO), 2.11−2.16 (m, 2H, CH_2 ring, β to CO), 2.50−2.53 (m, 2H, NCH_2 ring), 3.08−3.13 (m, 2H, NCH_2 ring), 3.37−3.44 (m, 2H, C*H), 3.65 (s, 6H, $2CH_3$), 3.76 (d, AB, 2H, ^2J = 13.8 Hz, ArCH_2N), 4.01 (d, AB, 2H, ^2J = 13.8 Hz, ArCH_2N), 7.32 (t, 1H, ^3J = 7.5 Hz), 7.60 (d, ^3J = 7.8 Hz, 2H); $^{13}C\{^1H\}$ NMR ($CDCl_3$) δ 23.24 (CH_2 ring γ to CO), 29.29 (CH_2 ring β to CO), 51.61 (CH_3), 53.32 (NCH_2 ring), 58.38 (ArCH_2N), 65.14 (*C**), 121.46 (Pyr *C*(*3*,*5*)), 136.76 (Pyr *C* (*4*)), 157.96 (Pyr *C* (*2*,*6*)), 174.53 (*C*O); UV−vis (MeCN) [λ_{max}, nm (ϵ, M^{-1} cm^{-1})] 214 (5495), 264 (4103).

[$FeCl_2$(Py(ProMe)$_2$)] (1). A colorless solution of anhydrous $FeCl_2$ (2.8 mmol, 350 mg) in dry MeOH (10 mL) was added to a slightly orange solution of **Py(ProMe)$_2$** (2.8 mmol, 1 g) dissolved in dry MeOH (10 mL). Immediately after addition, a color change of the reaction mixture to bright yellow was observed. The reaction mixture was stirred for 1 h at ambient temperature followed by evaporation of the solvent in vacuo. The remaining orange oil was dissolved in a minimum amount of dry MeOH and after addition of dry Et_2O (60 mL); the product precipitated as a yellow solid in 92% yield (1.23 g). Crystals suitable for X-ray diffraction were obtained within a few hours after addition of an excess of dry Et_2O

(16) Suter, G.; Stoykova, S. A.; Linden, A.; Heimgartner, H. *Helv. Chim. Acta* **2000**, *83*, 2961−2974.
(17) Paolucci, G.; Fischer, R. D.; Benetollo, F.; Seragli, R.; Bombieri, G. *J. Organomet. Chem.* **1991**, *412*, 327−342.
(18) Hagen, K. S. *Inorg. Chem.* **2000**, *39*, 5867−5860.

to a saturated metanolic solution of the complex. Anal. Calcd for $C_{19}H_{27}Cl_2FeN_3O_4$: C 46.75, H 5.57, N 8.61. Found: C 46.86, H 5.49, N 8.53. ESI-MS *m*/*z* 452 ((M − Cl)$^+$, calcd 452.1); $[\alpha]_D^{21}$ −48 deg cm^3 g^{-1} dm^{-1} (*c* 0.83, MeCN); IR (cm^{-1}, solid) ν 2951 (m), 2876 (m), 1731 (s), 1606 (m), 1579 (w), 1454 (w), 1434 (m), 1349 (w), 1213 (m), 1199 (m), 1174 (m), 1131 (m), 1109 (m), 1083 (m), 1028 (w), 984 (w), 984 (w), 791 (w); UV−vis (MeCN) [λ_{max}, nm (ϵ, M^{-1} cm^{-1})] 215 (10 591), 266 (6892), 343 (2646); CV (MeCN vs Fc/Fc$^+$) −0.099 V (ΔE = 98 mV).

[$ZnCl_2$(Py(ProMe)$_2$)] (2). A colorless solution of anhydrous $ZnCl_2$ (0.56 mmol, 76 mg) in dry MeOH (6 mL) was added to a slightly orange solution of **Py(ProMe)$_2$** (0.56 mmol, 200 mg) in dry MeOH (5 mL). The reaction mixture was stirred for 1 h at ambient temperature during which a white precipitate formed. The solid was collected by filtration and washed with MeOH. The product was isolated in 75% yield (203 mg). Slow cooling of a hot metanolic solution of the solid yielded colorless crystals suitable for X-ray diffraction. Anal. Calcd for $C_{19}H_{27}Cl_2ZnN_3O_4$: C 45.85, H 5.47, N 8.44. Found: C 45.95, H 5.61, N 8.38. ESI-MS *m*/*z* 460.05 ((M − Cl)$^+$, calcd 460.10); $[\alpha]_D^{21}$ −6.3 deg cm^3 g^{-1} dm^{-1} (*c* 1.025, MeCN); IR (cm^{-1}, solid) ν 2951 (m), 2873 (m), 1731 (s), 1609 (m), 1582 (w), 1467 (w), 1457 (w), 1434 (m), 1375 (w), 1349 (w), 1213 (m), 1199 (m), 1175 (m), 1139 (m), 1115 (m), 1086 (m), 1030 (w), 984 (w), 870 (w), 793 (m), 713 (w); ^{1}H NMR ($CDCl_3$) δ 1.91−1.99 (m, 4H, CH_2 ring, γ and β to CO), 2.22−2.27 (m, 2H, CH_2 ring, γ to CO), 2.55−2.63 (m, 2H, CH_2 ring, β to CO), 2.74 (q, 2H, ^3J = 9 Hz, NCH_2 ring), 3.09 (dt, 2H, ^3J = 3.9 and 9 Hz, NCH_2 ring), 3.72 (s, 6H, $2CH_3$), 4.10 (d, AB, 2H, ^2J = 14.7 Hz, ArCH_2N), 4.30 (d, AB, 2H, ^2J = 14.7 Hz, ArCH_2N), 4.69 (d, 2H, ^2J = 7.8 Hz, C*H), 7.31 (d, 2H, ^3J = 7.5 Hz), 7.91 (t, ^3J = 7.8 Hz, 1H); ^{13}C{^{1}H} NMR ($CDCl_3$) δ 22.80 (CH_2 ring γ to CO), 29.29 (CH_2 ring β to CO), 51.61 (CH_3), 51.99 (NCH_2 ring), 55.61 (ArCH_2N), 65.03 (*C**), 122.97 (Pyr *C* (*3,5*)), 141.49 (Pyr *C* (*4*)), 156.73 (Pyr *C* (*2,6*)), 173.70 (*C*O). UV−vis (MeCN) [λ_{max}, nm (ϵ, M^{-1} cm^{-1})] 215 (4281), 266 (5133).

[Fe(OTf)$_2$(Py(ProMe)$_2$)] (3). A colorless solution of Fe(OTf)$_2$·2MeCN (1.1 mmol, 483 mg) in MeCN (15 mL) was added to a slightly orange solution of Py(ProMe)$_2$ (1.1 mmol, 490 mg) dissolved in MeCN (15 mL). Immediately after addition, a color change of the reaction mixture to dark green was observed. The reaction mixture was stirred for 1 h at ambient temperature followed by evaporation of the solvent in vacuo. The remaining brown oil was dissolved in a minimal amount of dry MeCN and precipitated by addition of dry Et_2O (60 mL) as a green-yellow solid in 68% yield (540 mg). Crystals suitable for X-ray diffraction were obtained within a few hours after the addition of an excess of Et_2O to a saturated MeCN solution of the solid. Anal. Calcd for for $C_{21}H_{31}F_6FeN_3O_{12}S_2$: C 35.26, H 3.80, N 5.87. Found: C 35.08, H 3.86, N 5.78. ESI-MS *m*/*z* 566 ((M − OTf)$^+$, calcd 566.1); $[\alpha]_D^{21}$ −26 deg cm^3 g^{-1} dm^{-1} (*c* 0.9, MeCN); IR (cm^{-1}, solid) ν 2964 (w), 2886 (w), 1693 (s), 1609 (w), 1579 (w), 1449 (m), 1384 (m), 1355 (m), 1310 (w), 1278 (m), 1258 (m), 1236 (s), 1225 (s), 1159 (s), 1087 (w), 1056 (m), 1028 (s), 1028 (s), 945 (w), 926 (w), 876 (w), 846 (w), 796 (w), 760 (w); UV−vis (MeCN) [λ_{max}, nm (ϵ, M^{-1} cm^{-1})] 215 (6487), 265 (5150), 351 (574).

[Fe(Py(ProMe)$_2$(OH$_2$)$_2$](OTf)$_2$ (4). Complex **3** (0.156 mmol, 112 mg) was dissolved in CH_2Cl_2 (10 mL) followed by addition of water (1 mL), resulting in the formation of an orange precipitate. The reaction mixture was stirred vigorously at ambient temperature for 1 h. The upper water layer was removed by pipet and the organic layer containing the precipitate was evaporated in vacuo. The remaining orange solid was washed twice with CH_2Cl_2 (10 mL) and recrystallized from an acetonitrile (5 mL) solution with Et_2O (30 mL). The product was isolated as an orange solid in 77% yield (90 mg). The solid was dissolved in warm CH_2Cl_2, and slow evaporation of the solvent afforded crystals suitable for X-ray crystal structure determination. Anal. Calcd for for $C_{21}H_{31}F_6FeN_3O_{12}S_2$: C 33.57, H 4.16, N 5.59. Found: C 33.55, H 4.29, N 5.47. ESI-MS *m*/*z* 565.9 ((M − 2H$_2$O − OTf)$^+$, calcd 566.1), 208.5 ((M − 2H$_2$O − 2OTf)$^{2+}$, calcd 208.5); $[\alpha]_D^{21}$ −25 deg cm^3 g^{-1} dm^{-1} (*c* 0.6, MeCN); IR (cm^{-1}, solid) ν 3367 (br), 2962 (w), 1695 (s), 1608 (w), 1578 (w), 1448 (m), 1383 (w), 1353 (w), 1315 (sh), 1262 (sh), 1239 (s), 1226 (s), 1169 (s), 1100 (w), 1085 (w), 1052 (w), 1027 (s), 943 (w), 923 (w), 875 (w), 842 (w), 799 (w); UV−vis (MeCN) [λ_{max}, nm (ϵ, M^{-1} cm^{-1})] 215 (5603), 265 (4192), 351 (951).

[Zn(OTf)(Py(ProMe)$_2$)](OTf) (5). A colorless solution of anhydrous Zn(OTf)$_2$ (5.26 mmol, 190 mg) in dry MeOH (8 mL) was added to a slightly orange solution of **Py(ProMe)$_2$** (5.26 mmol, 190 mg) dissolved in dry MeOH (7 mL). The reaction mixture was stirred for 1 h at ambient temperature, and the solvent was evaporated in vacuo. The remaining pinkish oil was redissolved in a minimal amount of CH_2Cl_2, and the product was precipitated with Et_2O (50 mL). The product was isolated in 60% yield (224 mg) as a white solid. Crystals suitable for X-ray diffraction were obtained by slow diffusion of Et_2O into a methanolic solution of the solid. Anal. Calcd for $C_{21}H_{27}F_6S_2ZnN_3O_{10}$: C 34.79, H 3.75, N 5.80. Found: C 34.64, H 3.86, N 5.68. ESI-MS *m*/*z* 573.9 ((M − OTf)$^+$, calcd 574.1); $[\alpha]_D^{21}$ −25 deg cm^3 g^{-1} dm^{-1} (*c* 0.84, MeCN); IR (cm^{-1}, solid) ν 2966 (w), 2881 (w), 1676 (s), 1609 (w), 1589 (w), 1474 (w), 1449 (m), 1375 (m), 1319 (m), 1262 (s), 1244 (s), 1223 (s), 1153 (s), 1102 (m), 1076 (m), 948 (w), 876 (w), 792 (w); ^{1}H NMR (CD_3CN) δ 2.00−2.17 (m, 4H, CH_2 ring, γ and β to CO), 2.20−2.25 (m, 2H, CH_2 ring, γ to CO), 2.45−2.55 (m, 2H, CH_2 ring, β to CO), 3.13 (q, 2H, ^3J = 6.6 and 10.8 Hz, NCH_2 ring), 3.67 (quintet, 2H, ^3J = 5.4 Hz, NCH_2 ring), 3.74−3.79 (m, 2H, C*H), 3.81 (s, 6H, $2CH_3$), 4.17 (d, AB, 4H, ^2J = 16 Hz, ArCH_2N), 4.25 (d, AB, 4H, ^2J = 16 Hz, ArCH_2N), 7.42 (d, 2H, ^3J = 7.8 Hz), 8.02 (t, ^3J = 7.5 Hz, 1H); ^{13}C{^{1}H} NMR (CD_3CN) δ 25.80 (CH_2 ring γ to CO), 30.88 (CH_2 ring β to CO), 56.20 (NCH_2 ring), 58.35 (ArCH_2N), 61.59 (CH_3), 68.95 (*C**), 123.81 (Pyr *C* (*3,5*)), 142.90 (Pyr *C* (*4*)), 153.08 (Pyr *C* (*2,6*)), 182.74 (*C*O); UV−vis (MeCN) [λ_{max}, nm (ϵ, M^{-1} cm^{-1})] 215 (4763), 266 (5391).

Conductivity Measurements. The conductivity measurements were performed using a Consort C832 multimeter analyzer at ambient temperature. The measurements for compounds **1**, **3**, **4**, and **5** was carried out under nitrogen. The conductometer was calibrated using aqueous potassium chloride solutions. Procedure followed: first, the relative conductivity (κ in S cm^{-1}) of the solvent was measured (V = 10 mL), and then the relative conductivity of the samples with a concentration of ∼1 mM (V = 10 mL) was measured. The conductivity of the compound is obtained by subtraction of the blank conductivity from the conductivity of the sample. Molar conductivities (Λ_M in S cm^2 mol^{-1}) were calculated using the following equation: $\Lambda_M = 1000(\kappa/c)$.[19]

X-ray Crystal Structure Determinations. Crystals of compounds **1**−**5** suitable for X-ray crystallographic analysis were obtained as described (vide supra). X-ray intensities were measured on a Nonius Kappa CCD diffractometer with rotating anode (graphite monochromator, λ = 0.710 73 Å). The structures were solved with automated Patterson methods[20] (compounds **1**, **2**, and

(19) Atkins, P. W. *Physical Chemistry*, 5th ed.; Oxford University Press: Oxford, 1994; pp 834−841.

(20) Beurskens, P. T.; Admiraal, G.; Beurskens, G.; Bosman, W. P.; Garcia-Granda, S.; Gould, R. O.; Smits, J. M. M.; Smykalla, C. *The DIRDIF99 program system*; Technical Report of the Crystallography Laboratory, University of Nijmegen: Nijmegen, The Netherlands, 1999.

Table 1. Crystallographic Data for Compounds **1**−**5**

compound	**1**	**2**	**3**	**4**	**5**
formula	$C_{19}H_{27}Cl_2FeN_3O_4$	$C_{19}H_{27}Cl_2N_3O_4Zn$	$C_{21}H_{27}F_6FeN_3O_{10}S_2$	$C_{19}H_{31}FeN_3O_6{\cdot}2CF_3O_3S$	$C_{20}H_{27}F_3N_3O_7SZn{\cdot}CF_3O_3S$
fw	488.19	497.71	715.43	751.46	724.95
cryst color	yellow	colorless	yellow	red	colorless
cryst size [mm^3]	0.48 × 0.36 × 0.27	0.30 × 0.18 × 0.12	0.54 × 0.09 × 0.09	0.36 × 0.33 × 0.12	0.30 × 0.10 × 0.10
temp [K]	150	210	150	150	150
cryst syst	orthorhombic	orthorhombic	orthorhombic	monoclinic	monoclinic
space group	$P2_12_12_1$ (No. 19)	$P2_12_12_1$ (No. 19)	$P2_12_12_1$ (No. 19)	$P2_1$ (No. 4)	$P2_1$ (No. 4)
a [Å]	11.9312(1)	11.805(5)	9.0393(6)	9.6431(7)	9.7266(4)
b [Å]	13.6044(1)	13.723(3)	13.0683(13)	13.9031(12)	11.7644(5)
c [Å]	14.1521(1)	14.181(7)	24.218(3)	11.4677(12)	12.5504(6)
β [deg]	90	90	90	99.851(9)	92.7912(17)
V [Å^3]	2297.12(3)	2297.2(16)	2860.8(5)	1514.8(2)	1434.41(11)
Z	4	4	4	2	2
D_x [g/cm^3]	1.412	1.439	1.661	1.648	1.678
μ [mm^{-1}]	0.918	1.330	0.770	0.736	1.098
abs. corr. range	0.79−0.88	0.64−0.85	0.66−0.93	0.80−0.92	0.80−0.90
reflns collected/unique	42 597/5260	30 196/4261	35 955/5315	23 587/6883	12 718/3492
(sin $\theta/\lambda)_{max}$ [Å^{-1}]	0.65	0.61	0.61	0.65	0.53
params/restraints	265/0	265/0	390/0	424/1	444/121
R1/wR2 [$I > 2\sigma(I)$]	0.0231/0.0537	0.0286/0.0609	0.0342/0.0657	0.0260/0.0638	0.0503/0.1153
R1/wR2 [all reflns]	0.0266/0.0554	0.0360/0.0646	0.0577/0.0732	0.0313/0.0655	0.0598/0.1225
S	1.025	1.061	1.044	1.044	1.046
Flack × parameter[23]	−0.007(9)	−0.016(10)	−0.017(15)	0.025(8)	−0.01(2)
$\rho_{min/max}$ [e/Å^3]	−0.23/0.24	−0.30/0.29	−0.30/0.60	−0.24/0.35	−0.57/0.63

3) or Direct Methods (SHELXS-97[21a] for **4** and SIR-97[21b] for **5**) and refined with SHELXL-97[21c] against F^2 of all reflections. Non-hydrogen atoms were refined with anisotropic displacement parameters. Hydrogen atoms were located in the difference Fourier map (compounds **1**, **3**, and **4**) or introduced in calculated positions (compounds **2** and **5**). Hydrogen atoms were refined as rigid groups with the exception of the water hydrogens in **4**, which were refined freely with isotropic displacement parameters. In **1**, the methyl group at C(20) was rotationally disordered. In **5**, one of the proline rings had puckering disorder and the coordinated triflate showed positional disorder. Drawings, geometry calculations, and checking for higher symmetry was performed with the PLATON[22] program. Further details are given in Table 1.

Results

Synthesis. The **Py(ProMe)$_2$** ligand was synthesized in enantiomerically pure form using a one step procedure (Scheme 1). Reaction of 5 equiv of methyl-L-prolinate with 2,6-bis(chloromethyl)pyridine in hot methanol under basic conditions for 16 h afforded the target ligand in 90% yield after purification by column chromatography. A 5-fold excess of methyl-L-prolinate was used to obtain the ligand in a higher yield at the expense of monosubstituted byproduct. When 2.5 equiv of methyl-L-prolinate were used, the yield dropped to 47%.

Metal complexes **1**−**5** were synthesized by mixing an equimolar amount of **Py(ProMe)$_2$** and a divalent iron or zinc salt in methanol or acetonitrile. Reaction of anhydrous iron or zinc dichloride with **Py(ProMe)$_2$** afforded the isostructural, neutral complexes **1** [$FeCl_2$(**Py(ProMe)$_2$**)] (yellow) and **2** [$ZnCl_2$(**Py(ProMe)$_2$**)] (white). Changing the counterion in this procedure to the weakly coordinating triflate resulted in the formation of iron complex **3** [$Fe(OTf)_2$(**Py(ProMe)$_2$**)] (green-yellow) and zinc complex **5** [Zn(OTf)(**Py(ProMe)$_2$**)](OTf) (white), respectively. These complexes were also obtained upon reaction of **Py(ProMe)$_2$** with $FeCl_2$ or $ZnCl_2$, respectively, followed by the addition of 2 equiv of Ag(OTf) and removal of insoluble AgCl(s) by filtration. Addition of water to a CH_2Cl_2 solution of **3** resulted in the immediate precipitation of **4** [Fe(**Py(ProMe)$_2$**)$(OH_2)_2$](OTf)$_2$ as an orange-colored powder. Except that **3** is moisture sensitive, the other complexes appeared to be relatively stable toward O_2 and moisture, but the iron complexes **1**, **3**, and **4** were kept under nitrogen atmosphere when stored for longer periods. Typically, these complexes were isolated in 60−90% yield after recrystallization. Complexes **1**−**5** were characterized by a variety of techniques including single-crystal X-ray structural determination, UV−vis spectroscopy, CD measurements, magnetic susceptibility, elemental analysis, and ESI-MS.

Structural Features of Fe and Zn Complexes 1−5 in the Solid State (X-ray Crystal Structures). Crystals suitable for X-ray diffraction were obtained for each of the five complexes, which allowed the full characterization of their structure in the solid state (for details see Experimental Section). It is important to note that complexes **1**−**5** were formed as single diastereoisomers of which the configuration will be discussed (vide infra). Relevant crystallographic data are presented in Table 1, and selected bond distances and angles are listed in Table 2.

[$FeCl_2$(Py(ProMe)$_2$)] (1) and [$ZnCl_2$(Py(ProMe)$_2$)] (2). The molecular structure of neutral **1** [$FeCl_2$(**Py(ProMe)$_2$**)] in the crystal is shown in Figure 2 together with a quaternion overlay plot of its molecular structure with that of zinc(II) complex **2**.

This overlay nicely shows the perfect isostructural nature of these complexes in the solid state. The metal ions in these complexes are five coordinate by two chloride anions and

(21) (a) Sheldrick, G. M. *SHELXS-97, Program for crystal structure solution*; University of Göttingen: Göttingen, Germany, 1997. (b) Altomare, A.; Burla, M. C.; Camalli, M.; Cascarano, G. L.; Giacovazzo, C.; Guagliardi, A.; Moliterni, A. G. G.; Polidori, G.; Spagna, R. *J. Appl. Crystallogr.* **1999**, *32*, 115−119. (c) Sheldrick, G. M. *SHELXL-97, Program for crystal structure refinement*; University of Göttingen: Göttingen, Germany, 1997.
(22) Spek, A. L. *J. Appl. Crystallogr.* **2003**, *36*, 7−13.
(23) Flack, H. D. *Acta Crystallogr.* **1983**, *A39*, 876−881.

Table 2. Selected Distances (Å) and Angles (deg) for Complexes **1**−**5**

	1 (M = Fe)	**2** (M = Zn)	**3** (M = Fe)	**4** (M = Fe)	**5** (M = Zn)
			Bond Length (Å)		
M−N(1)	2.0752(12)	2.0414(19)	2.142(2)	2.1783(16)	2.050(6)
M−N(2)	2.4274(12)	2.450(2)	2.498(3)	2.3344(14)	2.226(7)
M−N(3)	2.4109(12)	2.435(2)	2.332(2)	2.3527(17)	2.206(8)
M−Cl(1)/O(1)	2.2754(5)	2.2177(11)	2.1125(19)	2.2676(14)	2.092(6)
M−Cl(2)/O(3)	2.2833(4)	2.2264(9)	2.241(2)	2.2434(13)	2.148(6)
M−O(5)			2.145(2)	2.1111(15)	2.041(5)
M−O(8)/O(6)			2.204(2)	2.1101(15)	
			Bond Angles (deg)		
N(1)−M−N(2)	74.99(5)	75.19(8)	71.55(9)	72.33(5)	76.8(3)
N(1)−M−N(3)	74.84(5)	75.01(8)	74.09(9)	71.61(6)	77.9(3)
N(2)−M−N(3)	149.77(4)	150.13(7)	145.51(9)	143.88(5)	154.4(3)
Cl(1)/O(1)−M−Cl(2)/O(3)	126.004(19)	122.63(3)	74.34(8)	74.07(5)	174.6(2)
N(1)−M−Cl(1)/O(1)	119.46(3)	120.82(6)			95.5(2)
N(2)−M−Cl(1)/O(1)	93.68(3)	94.44(6)	71.07(8)	70.63(5)	81.3(3)
N(3)−M−Cl(1)/O(1)	99.33(3)	98.93(6)			97.5(3)
N(1)−M−Cl(2)/O(3)	114.53(4)	116.55(6)			88.8(2)
N(2)−M−Cl(2)/O(3)	99.98(3)	99.70(5)			103.0(3)
N(3)−M−Cl(2)/O(3)	94.23(3)	95.36(5)	70.48(8)	71.48(5)	80.2(3)
O(5)−M−O(8)/O(6)			178.98(9)	170.21(7)	
N(1)−M−O(5)					171.8(3)
O(1)−M−O(5)					89.3(2)
O(3)−M−O(5)					86.8(2)
N(2)−M−O(5)					97.4(3)
N(3)−M−O(5)					108.2(3)

by the mer η^3-bonded **Py(ProMe)$_2$** ligand through the pyridine nitrogen and the two methyl prolinate nitrogen donor atoms. The complexes have an irregular coordination geometry, which is not on the Berry-pseudorotation path between trigonal bipyramid and square pyramid.[24] This is due to the bis-ortho chelate bonding of the tridentate **Py(ProMe)$_2$** ligand having one (central) M−N bond in common. The methyl ester groupings of the prolinate rings are pointing away from the metal center and are positioned above and below the plane defined by the metal and the three nitrogen donor atoms. This orientation complements the noncrystallographic overall C_2 symmetry of the complexes around an axis passing along the M···N(1)···C(4) vector. In both complexes, the M−N(pyr) distance is significantly shorter than the M−N(pro) distances; Fe−N(pyr) = 2.0752(12) Å and Zn−N(pyr) = 2.0414(19) Å, compared to Fe−N(pro) = 2.4274(12), 2.4109(12) Å and Zn−N(pro) = 2.450(2), 2.435(2) Å, respectively. The central plane of the complexes comprises the metal atom, the pyridine nitrogen, and the two chlorine atoms with N(pyr)−M−Cl angles of 114.53(4)−126.004(19)° in **1** and 116.55(6)−122.63(3)° in **2**. The *transoid* angle between the prolinate nitrogens is not linear, but amounts to 149.77(4)° in **1** and 150.13(7)° in **2**. The methylene groups joining the pyridine and prolinate rings cause a torsional twisting of the pyridyl ring from the plane defined by the metal and the three nitrogen donor atoms by 15.78(7)° for **1** and 16.36(11)° for **2**. The two five-membered chelate rings have a puckered conformation. The stereogenic nitrogen centers (because of M−N coordination) have an S_N configuration (see Discussion section), while the complexes are formed stereoselectively as single diastereomers.[25] Both methyl prolinate rings in **1** and **2** have an envelope conformation with the stereogenic carbon atom bearing the ester moiety out of the plane defined by the remaining ring atoms.

[Fe(OTf)$_2$(Py(ProMe)$_2$)] (3). The reaction of **Py(ProMe)$_2$** with Fe(OTf)$_2$·2MeCN yields complex **3** which has a rather unusual seven-coordinated iron(II) center. This compound crystallizes as discrete molecules [Fe(OTf)$_2$(**Py(ProMe)$_2$**)]. The coordination geometry around the iron center can be best described as distorted pentagonal bipyramidal (pbp, Figure 3). The equatorial plane of the bipyramid is occupied by the three nitrogen atoms of the ligand, as well as by the two oxygens of the carbonyl groups of the ester moieties, giving rise to four joined five-membered chelate rings. The two axial positions are occupied by the monodentate, η^1-O bonded triflate anions. The distortion of the pbp geometry in **3** is reflected in small deviations of all six atoms from the least-squares plane defined by the NN′NOOFe atoms (Fe(1) = 0.0580(4) Å, N(1) = −0.159(2) Å, N(2) = 0.177(2) Å, N(3) = −0.046(2) Å, O(1) = −0.243(2) Å and O(3) = 0.159(2) Å). The Fe−N distances significantly differ from each other, reflecting the different chemical nature of the nitrogen donor atoms. The Fe−N(pro) distances are distinctly longer (Fe−N(3) = 2.332(2) Å and Fe−N(2) = 2.498(3) Å) than the Fe−N(pyr) distance (Fe−N(1) = 2.142(3) Å). The Fe−N(2) distance is much longer than the Fe−N(3) distance and is in fact on the edge of what may be considered an Fe−N(sp^3) coordination bond length.[26] The free electron pair on N(2) is pointing toward the metal center, and its bonding most likely seems to be a consequence of the in-plane coordination of the other donor atoms of the ligand. The short Fe−O distance, i.e., that between iron and carbonyl

(24) Addison, A. W.; Rao, T. N.; Reedijk, J.; van Rijn, J.; Verschoor, G. C. *J. Chem. Soc., Dalton Trans.* **1984**, 1345−1349.

(25) The *S* configuration of the C-stereogenic center present on the prolinate ring maintains during synthesis.

(26) Orpen, A. G.; Brammer, L.; Allen, F. H.; Watson, D. G.; Taylor, R. *International Tables for Crystallography, Vol. C, Mathematical, Physical and Chemical Tables*, 3rd ed.; Prince, E., Ed.; Kluwer: Dordrecht, 2004.

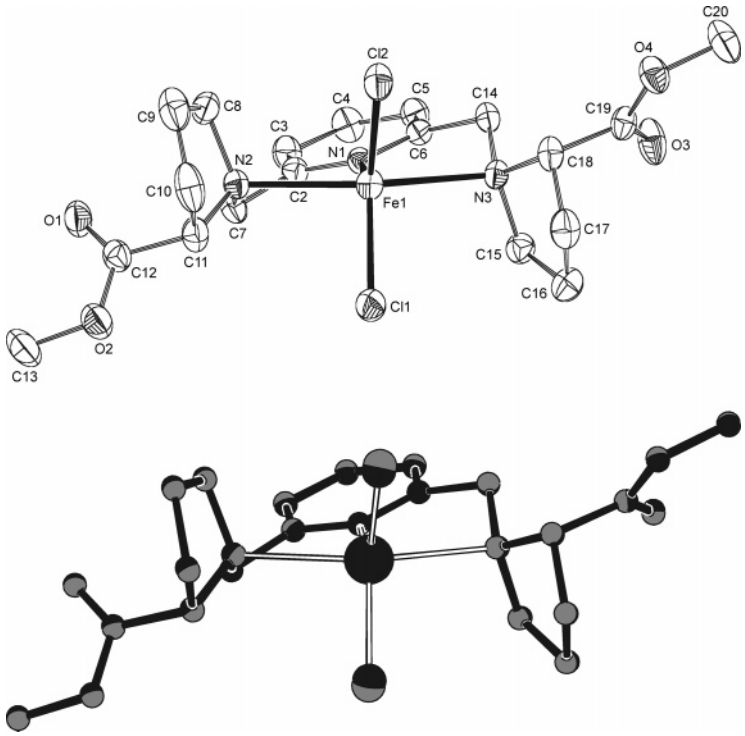

Figure 2. Top: Displacement ellipsoid plot (50% probability) of complex **1**, hydrogen atoms are omitted for clarity. Bottom: Quaternion fit of the isostructural complexes **1** and **2** (**1** drawn in gray, **2** in black).

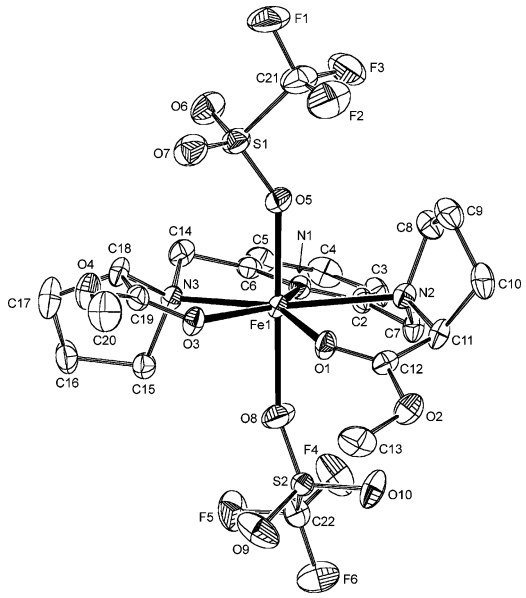

Figure 3. Displacement ellipsoid plot (50% probability) of **3**, [Fe(OTf)$_2$(**Py(ProMe)$_2$**)]; hydrogen atoms are omitted for clarity.

oxygen O(1) (2.1125(19) Å), seems to be the reason that N(2) is in the coordination sphere although at a long Fe−N(2) distance. The distance between iron and the second carbonyl oxygen amounts to Fe−O(3) = 2.241(2) Å, and the Fe−O distances of the axial η^1-bonded triflate oxygen atoms are Fe−O(5) = 2.145(2) Å and Fe−O(8) = 2.204(2) Å, respectively. The five angles subtended at iron by adjacent equatorial donor atoms of the four five-membered chelate rings deviate from the ideal value of 72°, having slightly smaller (71.55(9)°, 70.48(8)°, and 71.07(8)°) or higher (74.09(9)° and 74.34(8)°) values. However, the interaxial O(5)−Fe−O(8) angle (178.98(9)°) is very close to the ideal value of 180°. The torsional twisting of the pyridyl ring with respect to the pentagonal NN′NO$_2$ plane is 15.67(12)°. The distortion of **3** from an ideal pbp geometry is furthermore reflected in the different conformations of the five-membered chelate rings. The chelate ring Fe(1)−O(3)−C(19)−C(18)−N(3) has a half-chair conformation twisted around the N(3)−Fe(1) bond, while the Fe(1)−N(1)−C(6)−C(14)−N(3) chelate ring appears in an envelope conformation with N(3) out of the plane. Finally, both prolinate rings have an envelope conformation. In the ring containing N(2), C(9) is out of plane, whereas in the other ring the nitrogen atom N(3) appears to be out of the plane. As a result of these structural perturbations, the overall structure of **3** is devoid of any element of symmetry.

[Fe(Py(ProMe)$_2$)(OH$_2$)$_2$](OTf)$_2$ (4). The coordination of triflate anions in **3** is very labile. Upon exposure of **3** to moisture, the dicationic complex **4** is formed in which the coordinated triflate anions have been replaced by two water molecules while the two triflate anions appear as noncoordinating anions (Figure 4). The formal oxidation state of iron does not change in this process, nor does the overall coordination geometry around iron. The pentagonal bipyramidal geometry is actually less distorted in **4** than it is in **3**. The NN′NOO donor atoms and the iron center are essentially coplanar with a maximum deviation of 0.0597(14) Å observed for atom O(1). Selected distances and angles of **4** are summarized in Table 2. The change in coordination environment results in the elongation of the Fe−O(1) bond and subsequent shortening of the Fe−N(2) bond length. Now, the Fe−N(pro) distances in **4** are almost equal, which is in sharp contrast to the large differences seen in **3**. The Fe−N

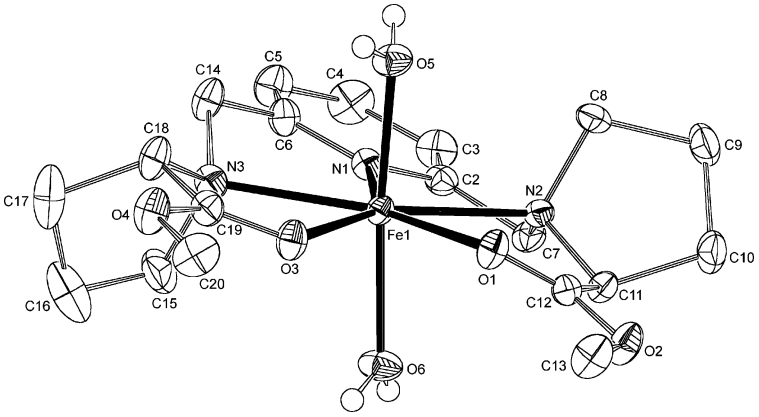

Figure 4. Displacement ellipsoid plot (50% probability) of cation of **4**, [Fe(**Py(ProMe)$_2$**)$(H_2O)_2$](OTf)$_2$; ligand hydrogen atoms and counteranions are omitted for clarity.

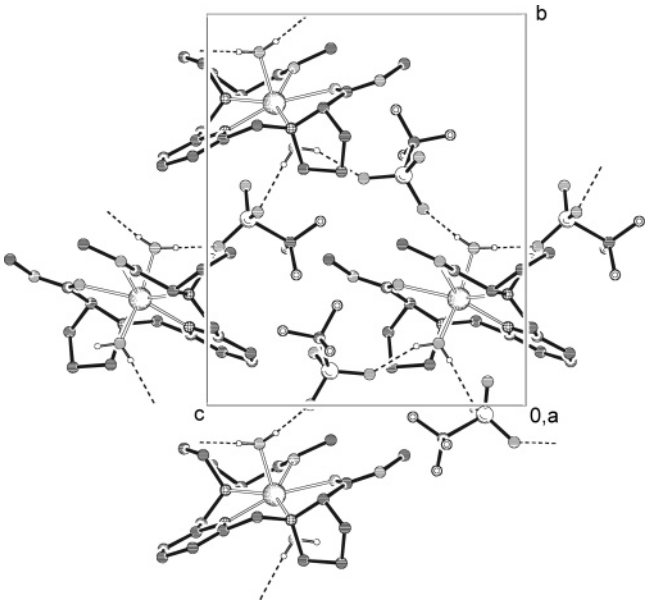

Figure 5. Packing of **4** in the crystallographic unit cell. View along the *a* axis. Dashed lines indicate hydrogen bonds between the water molecules as donors and the triflate anions as acceptors.

Table 3. Selected Hydrogen Bond Lengths (Å) and Angles (deg) of Complex **4**

donor−H···acceptor	D−H	H···A	D···A	D−H···A
O(5)−H(10)···O(9)	0.77(2)	1.96(2)	2.712(2)	167(2)
O(5)−H(20)···O(11)	0.85(3)	1.91(3)	2.752(2)	175(3)
O(6)−H(30)···O(12)	0.73(2)	2.02(3)	2.745(2)	175(2)
O(6)−H(40)···O(8)	0.80(5)	1.94(4)	2.690(3)	155(4)

distances in this complex also differ less than those observed in the other complexes, Fe−N(1) = 2.1783(16) Å, Fe−N(2) = 2.3344(14) Å, and Fe−N(3) = 2.3527(17) Å, respectively. The angles subtended around iron made up by the five adjacent equatorial atoms in **4** are close to the ideal value of 72° (72.33(5)°, 71.61(6)°, 71.48(5)°, and 70.63(5)°), with the exception of the O(1)−Fe−O(3) angle having a higher value of 74.07(5)°. The interaxial angle (O(5)−Fe−O(6) = 170.21(7)°) deviates from the ideal value of 180°. The torsional twisting of the pyridyl ring with respect to the equatorial plane has a slightly increased value of 17.53(8)°. The two prolinate rings appear in different conformations in **4**; the prolinate ring containing N(2) has an half-chair

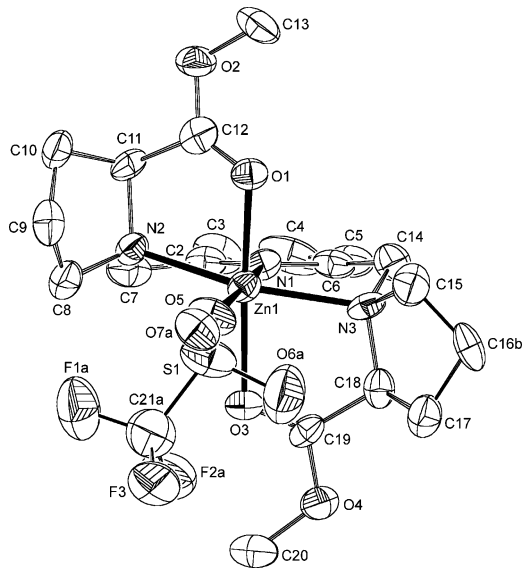

Figure 6. Displacement ellipsoid plot (50% probability) of **5**, [Zn(OTf)-(**Py(ProMe)$_2$**)](OTf); hydrogen atoms and the noncoordinated triflate are omitted for clarity. Only the major conformations of the disordered prolinate ring at C16 and of the disordered triflate are shown.

conformation twisted around the N(2)−C(8) bond, while the other ring containing N(3) appears in an envelope conformation with C(17) out of the plane. The coordinating water molecules are involved in a hydrogen-bonding network. Each triflate anion is bridging between two complexes, and every water molecule is involved in hydrogen bonding with two triflate anions (Figure 5, Table 3).

The prolinate nitrogen stereogenic centers in **3** and **4** have an R_N configuration which is opposite to the S_N configuration found in the iron dichloride complex **1**. The presence of strongly coordinated chloride anions in **1** and **2** forces the formation of complexes where the ester moieties are bend away to minimize the steric interaction with chloride anions. This results in the S_N configuration at the N-centers. The presence of weakly coordinating anions in **3**, **4**, and **5** (vide infra) results in stabilization of the metal center by coordination of the oxygen (carbonyl) atoms. This is only possible when the configuration of the nitrogen center is R_N, regardless of the geometry and coordination number around the metal ion.

Table 4. Selected Properties of **1**−**5** in the Solid State and in Acetonitrile Solution

complex **L** = **Py(ProMe)$_2$**	UV−vis[a] (λ_{max}, nm)	magnetic moment[b]	ν(CO)[b] (cm^{-1})	type of electrolyte[a]	configuration
[FeCl$_2$**L**] **1**	214 (2646), 266 (6892), 343 (2646)	5.21 μ_B	1731	neutral	$S_NS_NS_CS_C$
[ZnCl$_2$**L**] **2**	215 (4281), 266 (5133)	−	1731	neutral	$S_NS_NS_CS_C$
[Fe(OTf)$_2$**L**] **3**	215 (6487), 265 (5160), 351 (574)	4.91 μ_B	1693	2:1	$R_NR_NS_CS_C$
[Fe**L**(OH$_2$)$_2$](OTf)$_2$ **4**	215 (8410), 265 (6291), 351 (951)	4.93 μ_B	1695	2:1	$R_NR_NS_CS_C$
[Zn(OTf)**L**](OTf) **5**	215 (4763), 265 (5391),	−	1676	2:1	$R_NR_NS_CS_C$

[a] Measured in MeCN. Extinction coefficients are given in parentheses. [b] In the solid state.

[Zn(OTf)(Py(ProMe)$_2$)](OTf) (5). Selected bond distances and angles describing the molecular structure of **5** in the solid state, see Figure 6, are summarized in Table 2. Due to the disorder of the coordinated triflate anion, the overall C_2 symmetry of the complex is lost in the solid state. The equatorial plane of the distorted octahedron involves the three nitrogen atoms of the **Py(ProMe)$_2$** ligand and the η^1-bound oxygen atom of a monodentate bonded triflate anion. The NN′NO donor atoms and the zinc center are essentially coplanar with a maximum deviation of 0.094(6) Å for the pyridine nitrogen. The two axial positions are occupied by the oxygen atoms of the carbonyl groups of both ester moieties. The second triflate anion appears as a noncoordinating counterion. The difference in Zn−N distances in **5** is much smaller than has been observed for these bonds in the neutral, five-coordinate zinc dichloride complex **2**, Zn−N(1) = 2.050(6) Å, Zn−N(2) = 2.226(7) Å, and Zn−N(3) = 2.206(8) Å, respectively. The triflate-oxygen−zinc bond (Zn−O(5) = 2.041(5) Å) is shorter than the zinc distances to the (carbonyl) oxygen atoms in axial positions, Zn−O(1) = 2.092(6) Å and Zn−O(3) = 2.148(6) Å. The distortion of the octahedral geometry of **5** is reflected by the cisoid (76.8(3)−108.2(3)°) and transoid (154.4(3)°, 171.8(3)°, and 174.6(2)°) angles around the zinc atom. The torsional twist of the pyridyl ring from the equatorial plane of the metal with NN′NO donor atoms is 15.6(4)°. The five-membered chelate rings again appear in different conformations; the chelate formed by Zn(1)−N(1)−C(6)−C(14)−N(3) has a half-chair conformation twisted around the C(14)···N(3) bond, while the Zn(1)−N(1)−C(2)−C(7)−N(2) chelate appears in an envelope conformation with N(2) out of the plane. Both prolinate rings have an envelope conformation. In the ring containing N(2), C(9) is out of plane, and in the other ring containing N(3), both C(16A) and C(16B) are appearing out of the plane. The flexibility of the prolinate ring is observed in the prolinate ring with the N(3) atom in a puckering disorder of the C(16).

Finally, the magnetic moments of paramagnetic iron complexes **1**, **3**, and **4** (Table 4) were determined on a magnetic susceptibility balance at ambient temperature. Five-coordinate **1** and the two seven-coordinate complexes **3** and **4** showed magnetic moment values which are consistent with a high-spin electron configuration for the d^6 iron(II) center in these complexes (Table 4).

Structural Features of the Iron and Zinc Complexes 1−5 in Solution. To study the structural features of **1**−**5** in solution, ESI-MS, IR, conductivity, and UV−vis measurements on acetonitrile and/or dichloromethane solutions of these complexes were carried out. The analysis of **4** could only be performed in acetonitrile, as **4** is insoluble in dichloromethane. Complexes **1**−**5** remain mononuclear also in solution, as revealed by ESI-MS analysis of acetonitrile or dichloromethane solutions of **1**−**5**, showing the prominent cations [M(**Py(ProMe)$_2$**)X]$^+$ as the highest-molecular-weight species. Cyclic voltammetric measurements were also performed for the iron complexes **1**, **3**, and **4** in MeCN solutions. Complex **1** exhibits a (quasi) reversible one-electron wave (ΔE_P = 98 mV) with a half-wave potential value of −0.099 V vs Fc/Fc$^+$ for the Fe(II)/Fe(III) oxidation. Unfortunately, no diagnostic oxidative/reductive response was detected for complexes **3** and **4**, even though both complexes react with oxidants such as ROOH.[27] Complexes **2** and **5** were also analyzed by ^{1}H and ^{13}C{^{1}H} NMR spectroscopy.

Solid-State and Solution IR. The structural differences and coordination modes of the ligand in the iron and zinc complexes **1**−**5** are clearly reflected by their solid-state infrared spectra. The ν(C═O) of the five-coordinate complexes **1** and **2** (noncoordinated C═O in the solid state, Table 4) are identical with that of the parent ligand **Py(ProMe)$_2$**, i.e., 1731 cm^{-1}. In contrast, ν(C═O) of the complexes **3**, **4**, and **5** (coordinated C═O in the solid state) are shifted to lower frequencies (1693, 1695, and 1676 cm^{-1}, respectively, Table 4).

The IR experiments in solution were carried out on ∼15 mM samples of the respective complexes using ReactIR equipment at ambient temperature and under an inert nitrogen atmosphere using dry solvents (MeCN or CH_2Cl_2). The acetonitrile and dichloromethane solutions of the complexes **1** and **2** show ν(C═O)'s as were observed in their solid-state spectra. Comparison of the solution and solid-state IR data of the complexes **3**−**5** revealed some interesting solution behavior depending on the coordinating ability of the solvent.

(27) Gosiewska, S.; van Koten, G.; Klein Gebbink, R. J. M. Manuscript in preparation.

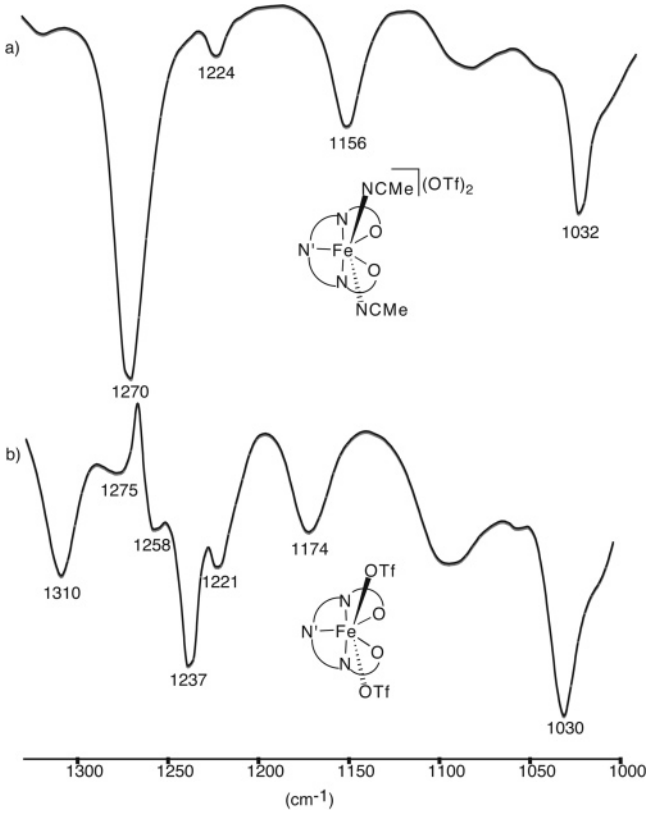

Figure 7. Solution IR spectra of complex **3** in (a) MeCN and (b) CH_2Cl_2.

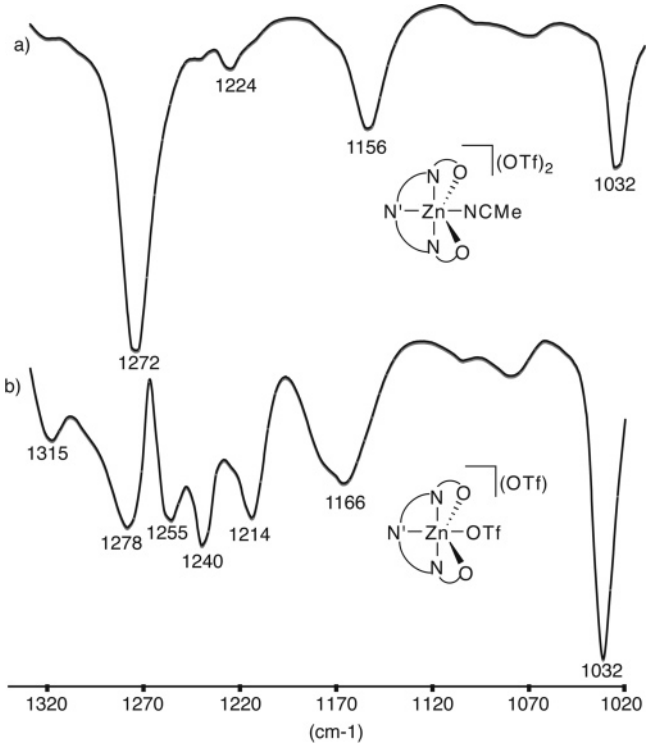

Figure 8. Solution IR spectra of complex **5** in (a) MeCN and (b) CH_2Cl_2.

In the solution IR spectra of **3**, the ν(C═O) slightly shifts from 1694 cm^{-1} in CH_2Cl_2 solution to 1687 cm^{-1} in MeCN solution. These data indicate that the coordination of the carbonyl groups (ν = 1693 cm^{-1}) as observed in the solid state for **3** is retained in both solvents. However, in the 1030−1310 cm^{-1} region where symmetric and asymmetric vibrations of the CF_3 and SO_3 groups appear, the acetonitrile and dichloromethane solution IR spectra of **3** differ significantly (Figure 7a). The presence of four sharp single vibrations at 1270 ($\nu_{as}SO_3$), 1224 (ν_sCF_3), 1156 ($\nu_{as}CF_3$), and 1032 cm^{-1} (ν_sSO_3) in acetonitrile solution (Figure 7a) indicates the presence of noncoordinated triflate anions,[28] i.e., of solvent-separated ion pairs (see Figure 10, vide infra). Supported by the appearance of a new vibration at 2254 cm^{-1} (ν(C≡N) of coordinated acetonitrile) we can indeed conclude that acetonitrile molecules have replaced both triflate anionic ligands in **3**, which thus appear as noncoordinated counteranions. The MeCN solutions of **3** and **4** gave essentially the same IR spectra, indicating that both complexes have the same coordination environment in a coordinating solvent like acetonitrile. In the noncoordinating solvent dichlomethane, the IR spectrum of a solution of **3** resembled the solid-state spectrum quite well. In dichloromethane solution, the symmetric SO_3 vibration shifts slightly to lower wavenumbers (1030 cm^{-1}), with respect to the $\nu_s(SO_3)$ observed in spectrum of **3** measured in MeCN, while two $\nu_{as}(SO_3)$ bands appear at 1237 and 1310 cm^{-1} (Figure 7b). The asymmetric SO_3 mode is now doubly degenerate, which can be assigned to two components resulting from triflate anion coordination.[29] Also, both vibrations for the CF_3 group shift to higher wavenumbers with respect of CF_3 vibrations observed in acetonitrile solution; 1174 (ν_{as} CF_3) and 1275 cm^{-1} (ν_s CF_3), respectively. These data support the view that, in CH_2Cl_2 solution, **3** retains its structural features found in the solid state, i.e., the anionic triflate ligands remain η^1-O coordinated. In the solid-state IR spectrum of **4**, vibrations at 1027 (ν_s SO_3), 1169 (ν_{as} CF_3), 1226 (ν_s CF_3), and 1239 cm^{-1} (ν_{as} SO_3) with two shoulders at 1262 and 1315 cm^{-1} appear because the "free" triflate anions have fixed positions due to the hydrogen bonds with coordinated water molecules and, therefore, show similar vibrations as for coordinated triflate anions.

The MeCN and CH_2Cl_2 IR spectra of the six-coordinate zinc complex **5** showed similar features as observed for complex **3** (Figure 8). The ν(CO) of the carbonyl group appears at 1677 cm^{-1} in CH_2Cl_2 solution, at 1679 cm^{-1} in MeCN solution, and at 1676 cm^{-1} in the solid state, indicating that both carbonyl groups remain coordinated to zinc in solution, as observed for the molecular structure of **5** in the solid state. The spectrum of **5** in acetonitrile showed sharp single vibrations at 1272 ($\nu_{as}SO_3$), 1224 (ν_sCF_3), 1156 ($\nu_{as}CF_3$) and 1032 cm^{-1} (ν_sSO_3), indicating that both triflate anions are noncoordinating. Appearance of a vibration at 2249 cm^{-1} suggests coordination of an acetonitrile molecule to zinc, i.e., substitution of the η^1-O coordinated triflate by acetonitrile occurred. The IR spectrum of a solution of **5** in dichloromethane resembled the solid-state IR, however, showing better resolution of bands in the 1030−1310 cm^{-1}

(28) (a) Aresta, M.; Quaranta, E.; Albinati, A. *Organometallics* **1993**, *12*, 2032−2043. (b) Aresta, M.; Dibenedetto, A.; Amodio, E.; Papai, I.; Schubert, G. *Inorg. Chem.* **2002**, *41*, 6550−6552.

(29) Bergström, P.-Å.; Frech, R. *J. Phys. Chem.* **1995**, *99*, 12603−12611.

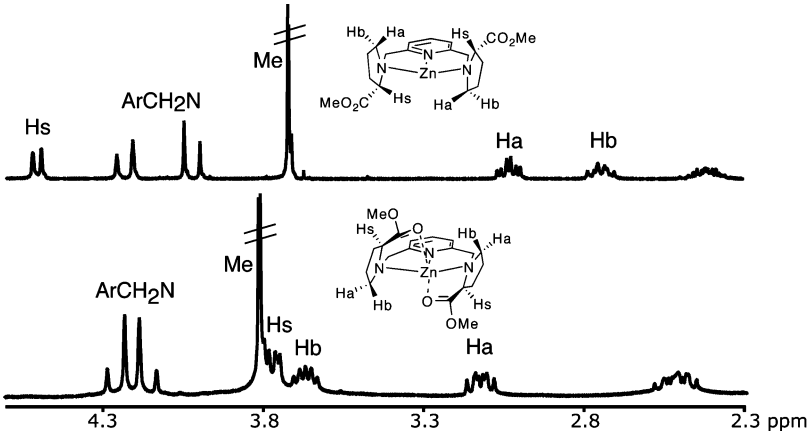

Figure 9. Selected part of the ^{1}H NMR spectra of zinc complexes **2** (top) and **5** (bottom) in CD_3CN with assignment of the most relevant protons.

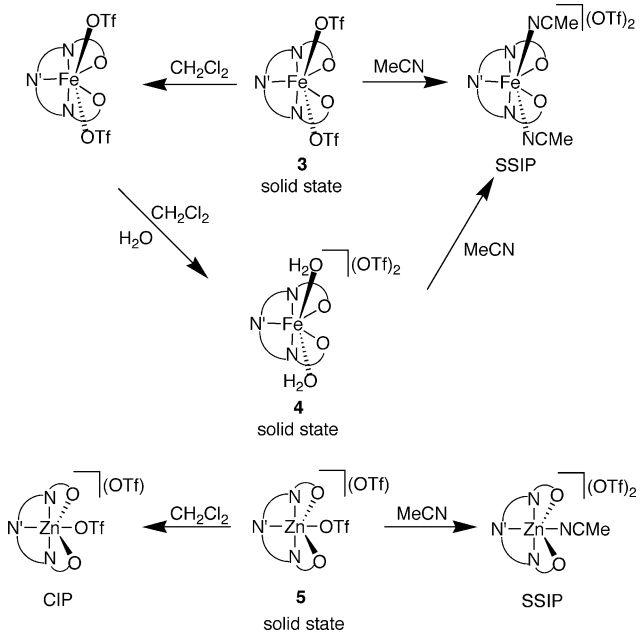

Figure 10. Summary of solution structures of complexes **3**−**5**. SSIP = solvent sepatated ion pair, CIP = contact ion pair.

region. The $\nu_{sym}(SO_3)$ appears at the same wavenumber (1032 cm^{-1}) but the $\nu_{as}(SO_3)$ splits into two bands at 1240 and 1315 cm^{-1} as a result of the coordination of one triflate anion to the zinc center. Both vibrations for the CF_3 group shift to higher wavenumbers, 1166 ($\nu_{as}CF_3$) and 1277 cm^{-1} (ν_sCF_3). The broad feature of $\nu_{as}(CF_3)$ together with the presence of vibrations at 1214 and 1255 cm^{-1} which can be assigned to $\nu_s(CF_3)$ and $\nu_{as}(SO_3)$ of a noncoordinated triflate anion, show that in CH_2Cl_2 one triflate is coordinated to zinc, while one remained noncoordinated as observed in the solid state.

Conductivity Measurements. The molar conductivities of **1**−**5** measured in acetonitrile, dichloromethane, and/or methanol at 1 mM concentrations (Table 5) support the assignments of the solution structures (vide supra). Very low molar conductivities of 47.1 and 6.1 S cm^2 mol^{-1} were found for complexes **1** and **2**, respectively, in MeCN, which supports the neutral nature of these [MCl_2(**Py(ProMe)$_2$**)] complexes. The slightly higher values for iron complex **1** can be compared to those reported for similar neutral dichloro iron complexes with nitrogen-based ligands, with molar

Table 5. Molar Conductivities of **1**−**5** Measured at Ambient Temperature

complex **L** = **Py(ProMe)$_2$**	molar conductivity (S cm^2 mol^{-1})[a]	
	MeCN	CH_2Cl_2
[$FeCl_2$**L**] **1**	47(1.02)	
[$ZnCl_2$**L**] **2**	6(1.03)	
[Fe(OTf)$_2$**L**] **3**	226(1.09)	4(1.1)
[Fe**L**$(OH_2)_2$][OTf)$_2$ **4**	258(1.13)	
[Zn(OTf)**L**](OTf) **5**	255(1.08)	11(1.1)

[a] The molar concentrations (mM) are given in parentheses after each feature.

conductivities between 30 and 62 S cm^2 mol^{-1}.[30,31] Complexes **3**−**5** gave high values of molar conductivities in acetonitrile, indicating a 2:1 electrolyte behavior.[32] In contrast to this ionic behavior in MeCN, in a noncoordinating solvent like CH_2Cl_2, the molar conductivity of **3** is well below the characteristic range for 1:1 electrolytes (19−22 S cm^2 mol^{-1}),[32] indicating the presence of a neutral complex. The molar conductivity of **5** in dichloromethane lies closer to the literature value for 1:1 electrolytes, which means that the structure in solution is essentially the same as the one found in the solid state.

UV−**Vis Measurements.** The UV−vis spectra of all complexes in MeCN show strong ligand-based absorptions around 215 and 265 nm (Table 4). These are the only absorption features present in the spectra of zinc complexes **2** and **5**. The iron complexes exhibit additional metal-to-ligand charge transfer (MLCT) bands at 343 nm (ϵ = 2646 M^{-1} cm^{-1}) for **1** and at 351 nm (ϵ = 574 M^{-1} cm^{-1} and ϵ = 951 M^{-1} cm^{-1}) for **3** and **4**, respectively.

NMR Analysis of 2 and 5. The IR and UV−vis analyses indicate the presence of a single species in solution for complexes **1**−**5**. The ^{1}H and $^{13}C\{^1H\}$ NMR spectra of zinc complexes **2** and **5** at room temperature showed the presence of a single species with an overall C_2 symmetry for each complex. Variable-temperature NMR measurements on **2**

(30) Hubin, T. J.; McCormick, J. M.; Collinson, S. R.; Buchalova, M.; Perkins, C. M.; Alcock, N. W.; Kahol, P. K.; Raghunatan, A.; Busch, D. H. *J. Am. Chem. Soc*. **2000**, *122*, 2512−2522.
(31) Mandon, D.; Machkour, A.; Goetz, S.; Welter, R. *Inorg. Chem*. **2002**, *41*, 5364−5372.
(32) (a) Uguagliatti, P.; Deganelo, G.; Busetto, L.; Belluco, U. *Inorg. Chem*. **1969**, *8*, 1625−1630. (b) Geary, W. J. *Coord. Chem. Rev*. **1971**, *7*, 81−122.

($CDCl_3$, temperature range of −60 to +60 °C) and **5** (CD_3CN, temperature range of −45 to +75 °C) showed no significant changes of the single resonance pattern. This indicates that also on the NMR time scale both zinc complexes exist as single diastereoisomers in solution.[33] The ^1H NMR resonance patterns of **2** and **5** in CD_3CN solution showed distinct differences (Figure 9). To fully assign the spectral features, 2D experiments ($^1H-^1H$ COSY and $^1H-^{13}C$ HETCOR) were performed. The stereogenic hydrogens (Hs) and the methylene hydrogens (Ha and Hb) next to the prolinate nitrogen are the most sensitive ones to reveal geometry differences of these two complexes. The stereogenic hydrogens in **2** point toward the $ZnCl_2$ fragment and have been shifted to lower field ($\delta = 4.49$) with respect to the free ligand. However, as a consequence of the Zn−O coordination in **5**, the stereogenic hydrogens are pointing away from the metal plane and their resonance appears at higher field ($\delta = 3.75$). Different multiplicities were observed for these protons in **2** and **5**, which could be a consequence of the different envelope of the prolinate ring leading to different coupling constants with neighboring CH_2 protons (J_{H-H}). The Hs multiplet observed in spectra of the parent ligand **Py(ProMe)$_2$** and **5** changed into a doublet in the spectrum of **2**. The hydrogens of the prolinate methylene group next to the nitrogen for both complexes appear as two separated resonances with different multiplicities, reflecting the diastereotopicity of these hydrogen atoms. The hydrogens pointing toward zinc, (Ha) in **2** and (Hb) in **5**, are shifted downfield compared to the other geminal hydrogens, (Hb) in **2** and (Ha) **5**. The different geometries (five-coordinate in **2** vs octahedral in **5**) of these complexes cause different relative orientations of the methylene group with respect to the metal (see Figures 2 and 6), which apparently results in downfield shift of both resonances in **5** ($\delta = 3.62$ and 3.13) compared to those in **2** ($\delta = 2.74$ and 3.09).

Discussion

Structural Considerations. Depending on the nature of the co-ligands, Cl^-, OTf^-, H_2O, or MeCN, the novel chiral **Py(ProMe)$_2$** ligand shows a high degree of flexibility in adopting different geometries and coordination modes (NN′N, NN′NO_2) when binding to either d^6 Fe(II) or d^{10} Zn(II). In the case of strongly coordinating and nucleophilic ligands, i.e., chloride anions, **Py(ProMe)$_2$** binds as a tridentate meridional ligand, yielding the five-coordinate neutral complexes **1** and **2**. In presence of weakly coordinating and nonnucleophilic ligands, i.e., OTf^- or H_2O, the **Py(ProMe)$_2$** ligand binds the metal centers in a pentadentate fashion. Besides the NN′N atoms of the ligand, the iron(II) center is stabilized by the coordination of the carbonyl groups of the ester moieties forming essentially a planar pentagon (NN′NO_2) around the metal ion with two η^1-O bonded triflate anions in the axial positions of a pentagonal bipyramid as in complex **3**. Whereas the equatorial ligands experience strong binding because of ligand field stabilization, the axial ligands are very labile and can be substituted easily. This is indeed observed for complex **3**. In the presence of moisture, the two coordinated triflate anions are readily replaced by two water molecules, forming complex **4**. As the d^{10} zinc(II) cation is not sensitive toward ligand field stabilization, a more common octahedral coordination geometry is adopted for **5** with the three nitrogen donor atoms in the plane with the carbonyl groups now coordinating in the axial positions. The remaining sixth site is occupied by a monodentate binding triflate anion. The coordination chemistry of the **Py(ProMe)$_2$** ligand as outlined here is summarized in Figure 10.

A number of iron and zinc metal complexes with general formula [MCl_2NN′N], containing a central pyridine (N′) moiety have been reported in the literature.[34] Out of these complexes, only three iron(II)[35] and two zinc(II)[36] X-ray structures have been reported that contain two sp^3 nitrogen-donor substituents next to the pyridine moiety. Common features of these five-coordinate complexes are the significantly shorter M−N(pyridyl) bond with respect to the M−N(sp^3) bonds, thereby reflecting the different nature of the nitrogen atoms. The much longer M−N(pro) distances in the isostructural complexes **1** and **2** than those observed for the previously reported [MCl_2NN′N] complexes can be explained by the increased basicity of the prolinate nitrogen compared to the dimethylamino nitrogen centers[36] and to the bulkiness of the **Py(ProMe)$_2$** ligand. The latter factor, together with the chelate coordination of the ligand, is

(33) The presence of different diastereoisomers in solution would be observed by ^1H and $^{13}C\{H\}$ spectroscopy. This was the case for related square planar NCN-pincer palladium bromide complexes already at ambient temperature. Gosiewska, S.; Huis in't Veld, M.; de Pater, J. J. M.; Bruijnincx, P. C. A.; Lutz, M.; Spek, A. L.; van Koten, G.; Klein Gebbink, R. J. M. *Tetrahedron: Asymmetry* **2006**, *4*, 674−686.

(34) For [$FeCl_2$NN′N] complexes, see: (a) Small, B. L.; Brookhart, M.; Bennet, A. M. A. *J. Am. Chem. Soc*. **1998**, *120*, 4049−4050. (b) Britovsek, G. P. J.; Gibson, V. C.; Kimberley, B. S.; Maddox, P. J.; McTavish, S. J.; Solan, G. A.; White, A. J. P.; Williams, D. J. *Chem. Commun*. **1998**, 849−850. (c) Small, B. L.; Brookhart, M. *J. Am. Chem. Soc*. **1998**, *120*, 7143−7144. (d) Britovsek, G. J. P.; Bruce, M.; Gibson, V. C.; Kimberley, B. S.; Maddox, P. J.; Mastroianni, S.; McTavish, S. J.; Redshaw, C.; Solan, G. A.; Strömberg, S.; White, A. J. P.; Williams, D. J. *J. Am. Chem. Soc*. **1999**, *121*, 8728−8740. (e) Britovsek, G. P. J.; Mastroianni, S.; Solan, G. A.; Baugh, S. P. D.; Redshaw, C.; Gibson, V. C.; White, A. J. P.; Williams, D. J.; Elsegood, M. R. J. *Chem. Eur. J*. **2000**, *6*, 2221−2231. (f) Suhr, D.; Lötscher, D.; Stoeckli-Evans, H.; von Zelewsky, A. *Inorg. Chim. Acta* **2002**, *341*, 17−24. For [$ZnCl_2$NN′N] complexes, see (g) Vlasse, M.; Rojo, T.; Beltran-Porter, D. *Acta Crystallogr., Sect. C: Cryst. Struct. Commun.* **1983**, *C39*, 560−563. (h) Birker, P. J. M. W. L.; Schierbeek, A. J.; Verschoor, G. C.; Reedijk, J. *J. Chem. Soc., Chem. Commun*. **1981**, 1124−1125. (i) Nicholson, G. A.; Petersen, J. L.; McCormick, B. J. *Inorg. Chem.* **1982**, *21*, 3274−3280. (j) Plenio, H.; Burth, D. *Organometallics* **1996**, *15*, 4054−4062. (k) Abufarang, A.; Vahrenkamp, H. *Inorg. Chem.* **1995**, *34*, 2207−2216. (l) Hazell, A.; McKenzie, C. J.; Nielsen, L. P. *J. Chem. Soc., Dalton Trans*. **1998**, 1751−1756. (m) Graf, M.; Greaves, B.; Stoeckli-Evans, H. *Inorg. Chim. Acta* **1993**, *204*, 239−246. (n) Amadei, E.; Carcelli, M.; Ianelli, S.; Cozzini, P.; Pelagatti, P.; Pelizzi, C. *J. Chem. Soc., Dalton Trans*. **1998**, 1205−1212. (o) Vance, A. L.; Alcock, N. W.; Heppert, J. A.; Busch, D. H. *Inorg. Chem.* **1998**, *37*, 6912−6920. (p) Smith, H. W. *Acta Crystallogr., Sect. B: Struct. Cryst. Chem.* **1975**, *B31*, 2701−2703. (q) Wirbser, J.; Vahrenkamp, H. *Z. Naturforsch. B: Chem. Sci.* **1992**, *47B*, 962−968. (r) Jiang, M.; Dalgarno, S.; Kilner, C. A.; Halcrow, M. A.; Kee, T. P. *Polyhedron* **2001**, *20*, 2151−2162.

(35) (a) Britovsek, G. J. P.; Gibson, V. C.; Mastroianni, S.; Oakes, D. C. H.; Redshaw, C.; Solan, G. A.; White, A. J. P.; Williams, D. J. *Eur. J. Inorg. Chem*. **2001**, 431−437. (b) Day, M. W.; Ward, B. D.; Grubbs, R. H. Private Communication to the Cambridge Structural Database, 2001, CCDC-133691. (c) O'Reilly, R. K.; Gibson, V. C.; White, A. J. P.; Williams, D. *Polyhedron* **2004**, *23*, 2921−2928.

(36) Del Río, I.; Gossage, R. A.; Hannu, M. S.; Lutz, M.; Spek, A. L.; van Koten, G. *Can. J. Chem*. **2000**, *78*, 1620−1626.

responsible for the irregular geometry around the metal centers in **1** and **2**.

Heptacoordinate Fe(II) complexes are rather unusual. It has been observed for pentadentate ligands comprising five donor atoms which are predisposed to provide planar pentadentate coordination and two nonnucleophilic coligands binding the axial position of a pentagonal bipyramidal (pbp) geometry.[37] Most of these Fe(II) complexes with pbp geometry are 2,6-diacetylpyridine diimine macrocyclic derivatives[37a−e] or crown ether derivatives.[37f,g] The X-ray structures of Fe(II) complexes with dipicolinic acid revealed the pbp geometry around the metal center, but the unit cell also contained mono-, di-, and trinuclear Fe(II) complexes.[38] The Fe(II) complexes of 1,3,5-triazine-2,4,6-tricarboxylate derivatives consist of one-dimensional chains composed of Fe(II) ions (with pbp geometry) and the triazine ligand in a 1:1 ratio.[39] Recently, Seitz et al. reported chiral, pentagonal bipyramidal Fe(II) complexes with a pentadentate binding bisoxazoline ligand.[40] $\pi-\pi$ stacking of the two phenyl moieties of the oxazoline substituents was the driving force for the formation of a P-helical structure. Among the reported complexes with pbp structures, only three complexes have an NN′NOO donor set comprising imine nitrogen donor atoms and with Cl^-, H_2O, or CN^- axial ligands.[37a,d,e] The small deviations from the basal MNN′NOO plane observed in **3** and **4** are comparable with those found in the pbp complexes reported in the literature. Due to the presence of benzylic methylene bridges a torsional twist of 15−17° for the pyridine ring from the MNN′NOO plane is observed. The Fe−N bond lengths above 2 Å present in the iron complexes **1** (five-coordinate), **3**, and **4** (seven-coordinate) point to the high-spin d^6 Fe(II) electron configurations of these complexes. This was confirmed by magnetic moment values of 4.91−5.21 μ_B which are comparable with the values found for structurally related five- or seven-coordinate iron(II) complexes.[34e,37d,e]

The presence of the benzylic methylene bridges, the sp^3 prolinate nitrogen atoms, and the nonplanar prolinate moieties seems to offer a high overall coordination flexibility to the **Py(ProMe)$_2$** ligand. One consequence of this flexibility is the formation of a six-coordinate Zn complex **5** with a more common octahedral geometry around the Zn(II) ion. Similar ligand flexibility in the formation of various zinc complexes with different coordination numbers, and hence geometries for the pentadentate ligand (2,6-bis{[(pyrid-2-ylmethyl)-amino]methyl}pyridine), was reported by Darbre et al.[41] However, for planar rigid pentadentate/heptadentate ligands lacking this flexibility, the formation of zinc(II) complexes with pbp geometry as found for the iron complexes **3** and **4** was reported, e.g., for 2,6-diacetylpyridine imine derivatives.[42]

Stereochemistry of the Complexes. Binding of the **Py(ProMe)$_2$** ligand to either zinc or iron creates a new stereogenic center on each prolinate nitrogen atom as a result of rather strong metal−prolinate nitrogen coordination. In principle, two enantiomeric pairs of diastereoisomer with R_NS_N/S_NR_N and R_NR_N/S_NS_N configurations (at the prolinate nitrogens) can form, resulting in a total of four unique diastereoisomers due to the presence of the Cα stereogenic centers (with a chosen and fixed *S* configuration) on the methyl-L-prolinate rings. However, a single diastereoisomer was found in the solid state for complexes **1**−**5** of which isostructural **1** and **2** have the $S_NS_NS_CS_C$ configuration and the complexes **3**, **4**, and **5** have the $R_NR_NS_CS_C$ configuration. The configuration of the prolinate nitrogens is determined by the coordination mode of the ligand. To minimize steric hindrance in the five-coordinate complexes **1** and **2**, both ester moieties are pointing away from the metal center, resulting in an S_N configuration. The formation of diastereoisomers with the opposite R_N configuration is a consequence of the coordination of the carbonyl groups to the metal in complexes **3**, **4**, and **5**. The relatively high coordination number of the metal centers in **1**−**5** (>4) seems to have a great influence on the preferential formation of the complexes as single diastereoisomers. This is apparent from the observation that structurally related NCN palladium halide complexes, in which the nitrogen donors of the tridentate NCN are also part of a methyl prolinate group, form all possible diastereoisomers in an equal ratio.[33] Besides the new stereogenic centers at the nitrogen atoms, also helical chirality at the metal center is generated upon formation of the metal **Py(ProMe)$_2$** complexes. The configuration created at the metal is defined by the nature of the coordination mode of

(37) (a) Palenik, G. J.; Wester, D. W. *Inorg. Chem*. **1978**, *17*, 864−870. (b) Bishop, M. M.; Lewis, J.; O' Donoghue, T. D.; Raithby, P. R.; Ramsden, J. N. *J. Chem. Soc., Dalton Trans.* **1980**, 1390−1396. (c) Dessy, G.; Fares, V. *Acta Cryst., Sect. C*: *Cryst. Struct. Commun*. **1981**, *10*, 1025−1028. (d) Bonardi, A.; Carini, C.; Merlo, C.; Pelizzi, C.; Pelizzi, G.; Tarasconi, P.; Vitali, F.; Cavatotra, F. *J. Chem. Soc., Dalton Trans.* **1990**, 2771−2777. (e) Hayami, S.; Gu, Z.-Z.; Einagi, Y.; Kobayasi, Y.; Ishikawa, Y.; Yamada, Y.; Fujishima, A.; Sato, O. *Inorg. Chem*. **2001**, *40*, 3240−3242. (f) Larson, S. B.; Simonsen, S. H.; Ramsden, J. N.; Lagowski, J. J. *Acta Crystallogr*. **1990**, *C46*, 1930−1932. (g) Atwood, J. L.; Junk, P. C. *Polyhedron* **2000**, 19, 85−91.

(38) Lainé, P.; Gourdon, A.; Launay, J.-P.; Tuchagues, J.-P. *Inorg. Chem.* **1995**, *34*, 5150−5155.

(39) Galán-Mascarós, J.-R.; Clemente-Juan, J.-M.; Dunbar, K. R. *J. Chem. Soc., Dalton Trans.* **2002**, 2710−2713.

(40) Seitz, M.; Kaiser, A.; Stempfhuber, S.; Zabel, M.; Reiser, O. *Inorg. Chem*. **2005**, *44*, 4630−4636.

(41) Darbre, T.; Dubs, C.; Rusanov, E.; Stoeckli-Evans, H. *Eur. J. Inorg. Chem*. **2002**, 3284−3291.

(42) (a) Wester, D.; Palenik, G. J. *J. Chem. Soc., Chem. Commun*. **1975**, 74−75. (b) Wester, D.; Palenik, G. J. *Inorg. Chem.* **1976**, *15*, 755−761. (c) Haque, Z. P.; Liles, D. C.; McPartlin, M.; Tasker, P. A. *Inorg. Chim. Acta* **1977**, *23*, L21−L22. (d) Liles, D. C.; McPartlin, M.; Tasker, P. A. *J. Chem. Soc., Dalton Trans.* **1987**, 1631−1636. (e) Adam, K. R.; Donnelly, S.; Leong, A. J.; Lindoy, L. F.; McCool, B. J.; Bashall, A.; Dent, M. R.; Murphy, B. P.; McPartlin, M.; Fenton, D. E.; Tasker, P. A. *J. Chem. Soc., Dalton Trans.* **1990**, 1635−1643. (f) Ianelli, S.; Minardi, G.; Pelizzi, C.; Pelizzi, G.; Reverberi, L.; Solinas, C.; Tarasconi, P. *J. Chem. Soc., Dalton Trans.* **1991**, 2113-2120. (g) Bino, A.; Cohen, N. *Inorg. Chim. Acta* **1993**, *210*, 11−16. (h) Rodriguez-Argüelles, M. C.; Bellicchi Ferrari, M.; Gasparri Fava, G.; Pelizzi, C.; Tarasconi, P.; Albertini, R.; Dall'Aglio, P. P.; Lunghi, P.; Pinelli, S. *J. Inorg. Biochem.* **1995**, *58*, 157−175. (i) de Souza, G. F.; Deflon, V. M. *Transition Met. Chem.* **2003**, *28*, 74−78. (j) Keypour, H.; Khanmohammadi, H.; Wainwright, K. P.; Taylor, M. R. *Inorg. Chim. Acta* **2003**, *355*, 286−291. (k) Kasuga, N. C.; Sekino, K.; Ishikawa, M.; Honda, A.; Yokoyama, M.; Nakano, S.; Shimada, N.; Koumo, C.; Nomiya, K. *J. Inorg. Biochem.* **2003**, *96*, 298−310. (l) Bencini, A.; Berni, E.; Bianchi, A.; Fornasari, P.; Giorgi, C.; Lima, J. C.; Lodeiro, C.; Melo, M. J.; Seixas de Melo, J.; Parola, A. J.; Pina, F.; Pina, J.; Valtancoli, B. *Dalton Trans*. **2004**, 2180−2187. (m) Matesanz, A. I.; Cuadrado, I.; Pastor, C.; Souza, P. *Z. Anorg. Allg. Chem*. **2005**, *631*, 780−784.

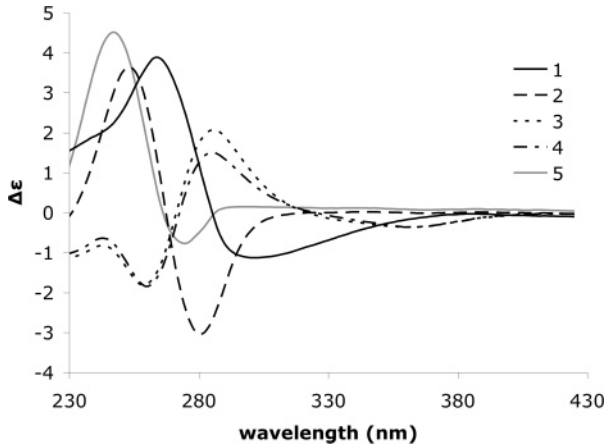

Figure 11. CD spectra in MeCN of complexes **1**−**5**.

the ligand (NN′N vs NN′NOO) and the positions of the prolinate rings with respect to the NN′NM plane. The assignment of the metal configuration in complexes **1**−**5** was rationalized on the basis of their solid-state structures, the sector rules for C_2-symmetric pyridine complexes reported by Palmer and co-workers,[43] and by comparison of their CD spectra with those of structurally related complexes reported in the literature.[44] For this reason, the solution CD spectra of complexes **1**−**5** were recorded in MeCN in the range of 230−400 nm (Figure 11). The simplest case is the octahedral complex **5**, showing a positive Cotton effect around 250 nm. From the solid-state structure (Figure 6), a Λ-configuration can be assigned; the prolinate ring containing N(2) is positioned above the NN′NM plane and the N(3) prolinate ring below the plane.

The five-coordinate complexes **1** and **2** also gave positive Cotton effects (∼270 nm (**1**) and 250 nm (**2**)) and the X-ray crystal structure reveals the same positioning of the prolinate rings as in **5**. Complexes **1** and **2**, therefore, also exhibit the Λ-configuration around the metal centers regardless of their opposite configuration of the nitrogen atoms as compared to **5**. The CD spectra of complexes **3** and **4** show a negative Cotton effect at 265 and 360 nm (weak). As the N(2) and N(3) prolinate rings are positioned in an opposite manner with respect to the NN′NM plane as compared to complex **5** (Figures 3 and 4), a Δ-configuration was assigned to complexes **3** and **4**. Apparently, the configuration of the Cα stereogenic centers and the overall geometry around the metal dictates the configuration at the metal centers. Since the complexes have different geometries and coordination numbers, their opposite diastereoisomers would be obtained only from the D-proline-derived ligands.

Conclusions

The structural analysis of a series of iron(II) and zinc(II) complexes of the novel chiral **Py(ProMe)$_2$** ligand demonstrates the intrinsic flexibility of this ligand to adopt different geometries depending on the metal and the coordination ability of counteranions. The η^3-NN′N meridional coordination of the **Py(ProMe)$_2$** ligand can be accompanied by additional coordination of the carbonyl-O donor atoms of the ligand to form robust metal complexes with defined geometries in the solid state and in solution. The straightforward and feasible synthesis of the ligand in an enantiomerically pure form and the structural integrity of its single diastereomeric metal complexes in solution make it an attractive and promising building block for the development of stereoselective catalysts. The essentially planar pentadentate coordination of the ligand around an iron center leaving the two axial positions available for substrates and/or reagents as was observed in complexes **3** and **4** is reminiscent of porphyrin-, salen-, and cyclam-type ligation modes. Studies on the oxidation reactivity of the iron complexes described herein are currently ongoing in our laboratory.

Acknowledgment. The work described here was financially supported by the National Research School Combination-Catalysis (NRSC-C) (S.G.) and the Council for Chemical Sciences of The Netherlands Organization for Scientific Research (CW-NWO) (M.L., A.L.S.). The authors acknowledge Dr. Lies Bouwman and Dr. Meenal Godbole (Leiden Institute of Chemistry) for using their magnetic susceptibility balance and their help with magnetic measurements.

Supporting Information Available: CIF files for the X-ray structural data of complexes **1**−**5**. This material is available free of charge via the Internet at http://pubs.acs.org.

IC060134Z

(43) Dyer, R. B.; Palmer, R. A.; Ghirardelli, R. G.; Bradshaw, J. S.; Jones, B. A. *J. Am. Chem. Soc*. **1987**, *109*, 4780−4786.

(44) (a) Bernauer, K.; Pousaz, P.; Porret, J.; Jeanguenat, A. *Helv. Chim. Acta* **1988**, *71*, 1339−1348. (b) Bernauer, K.; Stoeckli-Evans, H.; Hugi-Cleary, D.; Hilgers, H. J.; Abd-el-Khalek, H.; Porret, J.; Sauvain, J.-J. *Helv. Chim. Acta* **1992**, *75*, 2327−2339.